

CERN-EP-2019-189
2020/02/27

CMS-TOP-19-007

Running of the top quark mass from proton-proton collisions at $\sqrt{s} = 13$ TeV

The CMS Collaboration*

Abstract

The running of the top quark mass is experimentally investigated for the first time. The mass of the top quark in the modified minimal subtraction ($\overline{\text{MS}}$) renormalization scheme is extracted from a comparison of the differential top quark-antiquark ($t\bar{t}$) cross section as a function of the invariant mass of the $t\bar{t}$ system to next-to-leading-order theoretical predictions. The differential cross section is determined at the parton level by means of a maximum-likelihood fit to distributions of final-state observables. The analysis is performed using $t\bar{t}$ candidate events in the $e^{\pm}\mu^{\mp}$ channel in proton-proton collision data at a centre-of-mass energy of 13 TeV recorded by the CMS detector at the CERN LHC in 2016, corresponding to an integrated luminosity of 35.9 fb^{-1} . The extracted running is found to be compatible with the scale dependence predicted by the corresponding renormalization group equation. In this analysis, the running is probed up to a scale of the order of 1 TeV.

"Published in Physics Letters B as doi:10.1016/j.physletb.2020.135263."

1 Introduction

Beyond leading order in perturbation theory, the fundamental parameters of the quantum chromodynamics (QCD) Lagrangian, i.e. the strong coupling constant α_S and the quark masses, are subject to renormalization. As a result, these parameters depend on the scale at which they are evaluated. The evolution of α_S and of the quark masses as a function of the scale, commonly referred to as “running”, is described by renormalization group equations (RGEs). The running of α_S was experimentally verified on a wide range of scales using jet production in electron-proton, positron-proton, electron-positron, proton-antiproton, and proton-proton (pp) collisions, as summarized, e.g. in Refs. [1, 2]. To determine the running, the value of α_S evaluated at an arbitrary reference scale is extracted in bins of a physical energy scale Q and then converted to $\alpha_S(Q)$ using the corresponding RGE [2]. The validity of this procedure lies in the fact that, in a calculation, the renormalization scale is normally identified with the physical energy scale of the process. The same procedure can be used to determine the running of the mass of a quark. In the modified minimal subtraction ($\overline{\text{MS}}$) renormalization scheme, the dependence of a quark mass m on the scale μ is described by the RGE

$$\mu^2 \frac{dm(\mu)}{d\mu^2} = -\gamma(\alpha_S(\mu)) m(\mu), \quad (1)$$

where $\gamma(\alpha_S(\mu))$ is the mass anomalous dimension, which is known up to five-loop order in perturbative QCD [3, 4]. The solution of Eq. 1 can be used to obtain the quark mass at any scale μ from the mass evaluated at an initial scale μ_0 . The running of the b quark mass was demonstrated [5] using data from various experiments at the CERN LEP [6–9], SLAC SLC [10], and DESY HERA [11] colliders. Measurements of charm quark pair production in deep inelastic scattering at the DESY HERA were used to determine the running of the charm quark mass [12]. These measurements represent a powerful test of the validity of perturbative QCD. Furthermore, RGEs can be modified by contributions from physics beyond the standard model, e.g. in the context of supersymmetric theories [13].

This Letter describes the first experimental investigation of the running of the top quark mass, m_t , as defined in the $\overline{\text{MS}}$ scheme. The running of m_t is extracted from a measurement of the differential top quark-antiquark pair production cross section, $\sigma_{t\bar{t}}$, as a function of the invariant mass of the $t\bar{t}$ system, $m_{t\bar{t}}$. The differential cross section, $d\sigma_{t\bar{t}}/dm_{t\bar{t}}$, is determined at the parton level by means of a maximum-likelihood fit to distributions of final-state observables using $t\bar{t}$ candidate events in the $e^\pm\mu^\mp$ final state, extending the method described in Ref. [14] to the case of a differential measurement. This method allows the differential cross section to be constrained simultaneously with the systematic uncertainties. In this analysis, the parton level is defined before radiation from the parton shower, which allows for a direct comparison with fixed-order theoretical predictions. The measurement is performed using pp collision data at $\sqrt{s} = 13$ TeV recorded by the CMS detector at the CERN LHC in 2016, corresponding to an integrated luminosity of 35.9 fb^{-1} . The running mass, $m_t(\mu)$, is extracted at next-to-leading order (NLO) in QCD as a function of $m_{t\bar{t}}$ by comparing fixed-order theoretical predictions at NLO to the measured $d\sigma_{t\bar{t}}/dm_{t\bar{t}}$. The running of m_t is probed up to a scale of the order of 1 TeV.

2 The CMS detector and Monte Carlo simulation

The central feature of the CMS apparatus is a superconducting solenoid of 6 m internal diameter, providing a magnetic field of 3.8 T. Within the solenoid volume are a silicon pixel and strip

tracker, a lead tungstate crystal electromagnetic calorimeter (ECAL), and a brass and scintillator hadron calorimeter, each composed of a barrel and two endcap sections. Forward calorimeters extend the pseudorapidity (η) coverage provided by the barrel and endcap detectors. Muons are detected in gas-ionization chambers embedded in the steel flux-return yoke outside the solenoid. A two-level trigger system selects events of interest for analysis [15]. A more detailed description of the CMS detector, together with a definition of the coordinate system used and the relevant kinematic variables, can be found in Ref. [16].

The particle-flow (PF) algorithm [17] aims to reconstruct and identify electrons, muons, photons, charged and neutral hadrons in an event, with an optimized combination of information from the various elements of the CMS detector. The energy of electrons is determined from a combination of the electron momentum at the primary interaction vertex as determined by the tracker, the energy of the corresponding ECAL cluster, and the energy sum of all bremsstrahlung photons spatially compatible with originating from the electron track [18]. The momentum of muons is obtained from the curvature of the corresponding track [19]. Jets are reconstructed from the PF candidates using the anti- k_T clustering algorithm with a distance parameter of 0.4 [20, 21], and the jet momentum is determined as the vectorial sum of all particle momenta in the jet. The missing transverse momentum vector is computed as the negative vector sum of the transverse momenta (p_T) of all the PF candidates in an event. Jets originating from the hadronization of b quarks (b jets) are identified (b tagged) using the combined secondary vertex [22] algorithm, using a working point that corresponds to an average b tagging efficiency of 41% for simulated $t\bar{t}$ events, and an average misidentification probability of 0.1% and 2.2% for light-flavour jets and c jets, respectively [22].

In this analysis, the same Monte Carlo (MC) simulations as in Ref. [14] are used. In particular, $t\bar{t}$, tW , and Drell–Yan (DY) events are simulated using the POWHEG v2 [23–28] NLO MC generator interfaced to PYTHIA 8.202 [29] for the modelling of the parton shower and using the CUETP8M2T4 underlying event tune [30, 31]. In the simulation, the proton structure is described by means of the NNPDF3.0 [32] parton distribution function (PDF) set. The largest background contributions are represented by tW and DY production. Other background processes include W +jets production and diboson events, while the contribution from QCD multi-jet production is found to be negligible. Contributions from all background processes are estimated from simulation and are normalized to their predicted cross section. Further details on the MC simulation of the backgrounds can be found in Ref. [14].

3 Event selection and systematic uncertainties

Events are collected using a combination of triggers which require either one electron with $p_T > 12$ GeV and one muon with $p_T > 23$ GeV, or one electron with $p_T > 23$ GeV and one muon with $p_T > 8$ GeV, or one electron with $p_T > 27$ GeV, or one muon with $p_T > 24$ GeV. In the analysis, tight isolation requirements are applied to electrons and muons based on the ratio of the scalar sum of the p_T of neighbouring PF candidates to the p_T of the lepton candidate. Events are then required to contain at least one electron and one muon of opposite electric charge with $p_T > 25$ GeV for the leading and $p_T > 20$ GeV for the subleading lepton, and $|\eta| < 2.4$. This kinematic selection defines the visible phase space. In events with more than two leptons, the two leptons of opposite charge with the highest p_T are used. Jets with $p_T > 30$ GeV and $|\eta| < 2.4$ are considered, but no requirement on the number of reconstructed jets or b-tagged jets is imposed. Further details on the event selection can be found in Ref. [14].

In events with at least two jets, the invariant mass of the $t\bar{t}$ system is estimated by means of the kinematic reconstruction algorithm described in Ref. [33]. The reconstructed invariant mass is

indicated with $m_{t\bar{t}}^{\text{reco}}$. The kinematic reconstruction algorithm examines all possible combinations of reconstructed jets and leptons and solves a system of equations under the assumptions that the invariant mass of the reconstructed W boson is 80.4 GeV and that the missing transverse momentum originates solely from the two neutrinos coming from the leptonic decays of the W bosons. In addition, the kinematic reconstruction algorithm requires an assumption on the value of the top quark mass, m_t^{kin} . Any possible bias due to the choice of this value is avoided by incorporating the dependence on m_t^{kin} in the fit described in Section 4. To estimate this dependence, the kinematic reconstruction and the event selection are repeated with three different choices of m_t^{kin} , corresponding to 169.5, 172.5, and 175.5 GeV, and the top quark mass used in the MC simulation, m_t^{MC} , is varied accordingly. The parameter $m_t^{\text{kin}} = m_t^{\text{MC}}$ is then treated as a free parameter of the fit.

The sources of systematic uncertainties are classified as experimental and modelling uncertainties. Experimental uncertainties are related to the corrections applied to the MC simulation. These include uncertainties associated with trigger and lepton identification efficiencies, jet energy scale [34] and resolution [35], lepton energy scales, b tagging efficiencies [22], and the uncertainty in the integrated luminosity [36]. Modelling uncertainties are related to the simulation of the $t\bar{t}$ signal, and include matrix-element scale variations in the POWHEG simulation [37, 38], scale variations in the parton shower [31], variations in the matching scale between the matrix element and the parton shower [30], uncertainties in the underlying event tune [30], the PDFs [39], the B hadron branching fraction and fragmentation function [40, 41], and uncertainties related to the choice of the colour reconnection model [42, 43]. Furthermore, as in previous CMS analyses, e.g. [14, 44, 45], an uncertainty that accounts for the observed difference in the shape of the top quark p_T distribution between data and simulation [33, 46, 47] is applied. The dependence on the top quark width has been investigated and was found to be negligible. Other sources of uncertainty include the modelling of the additional pp interactions within the same or nearby bunch crossings and the normalization of background processes. For the latter, an uncertainty of 30% is assigned to the normalization of each background process. Further details on the sources of systematic uncertainties and the considered variations can be found in Ref. [14].

The simulated $t\bar{t}$ sample is split into four subsamples corresponding to bins of $m_{t\bar{t}}$ at the parton level. Each subsample is treated as an independent signal process, representing the $t\bar{t}$ production at the scale μ_k , which is chosen to be the centre-of-gravity of bin k , defined as the mean value of $m_{t\bar{t}}$ in that bin. The subsample corresponding to the bin k is denoted with “Signal (μ_k)”. The $m_{t\bar{t}}$ bin boundaries, the corresponding fraction of simulated events in each bin, and the representative scales μ_k are summarized in Table 1, where the values are estimated from the nominal POWHEG simulation. The width of each bin, $\Delta m_{t\bar{t}}^k$, is chosen taking into account the resolution in $m_{t\bar{t}}^{\text{reco}}$. Figure 1 shows the distribution of $m_{t\bar{t}}^{\text{reco}}$ after the fit to the data, which is described in the next section.

Table 1: The $m_{t\bar{t}}$ bin boundaries, the corresponding fraction of events in the POWHEG simulation, and the representative scale μ_k .

Bin	$m_{t\bar{t}}$ [GeV]	Fraction [%]	μ_k [GeV]
1	<420	30	384
2	420–550	39	476
3	550–810	24	644
4	>810	7	1024

4 Fit procedure and cross section results

The differential $t\bar{t}$ cross section at the parton level is measured by means of a maximum-likelihood fit to distributions of final-state observables where the systematic uncertainties are treated as nuisance parameters. In the likelihood, the number of events in each bin of any distribution of final-state observables is assumed to follow a Poisson distribution. With $\sigma_{t\bar{t}}^{(\mu_k)} = (d\sigma_{t\bar{t}}/dm_{t\bar{t}})\Delta m_{t\bar{t}}^k$ being the total $t\bar{t}$ cross section in the bin k of $m_{t\bar{t}}$, the expected number of events in the bin i of any of the considered final-state distributions, denoted with ν_i , can be written as

$$\nu_i = \sum_{k=1}^4 s_i^k(\sigma_{t\bar{t}}^{(\mu_k)}, m_t^{\text{MC}}, \vec{\lambda}) + \sum_j b_i^j(m_t^{\text{MC}}, \vec{\lambda}). \quad (2)$$

Here, s_i^k indicates the expected number of $t\bar{t}$ events in the bin k of $m_{t\bar{t}}$ and depends on $\sigma_{t\bar{t}}^{(\mu_k)}$, m_t^{MC} , and the nuisance parameters $\vec{\lambda}$. Similarly, b_i^j represents the expected number of background events from a source j and depends on m_t^{MC} and the nuisance parameters $\vec{\lambda}$. The dependence of the background processes on m_t^{MC} is introduced not only by the contribution of tW and semileptonic $t\bar{t}$ events, but also by the choice of m_t^{kin} in the kinematic reconstruction. Equation 2, which relates the various $\sigma_{t\bar{t}}^{(\mu_k)}$ (and hence the parton-level differential cross section) to distributions of final-state observables, embeds the detector response and its parametrized dependence on the systematic uncertainties. Therefore, the maximization of the likelihood function provides results for $\sigma_{t\bar{t}}^{(\mu_k)}$ that are automatically unfolded to the parton level. This method (described, e.g. in Ref. [48]) is also referred to as maximum-likelihood unfolding and, unlike other unfolding techniques, allows the nuisance parameters to be constrained simultaneously with the differential cross section. The unfolding problem was found to be well-conditioned, and therefore no regularization is needed. The expected signal and background distributions contributing to the fit are modelled with templates constructed using simulated samples.

Selected events are categorized according to the number of b-tagged jets, as events with 1 b-tagged jet, 2 b-tagged jets, or a different number of b-tagged jets (zero or more than two). The effect of the systematic uncertainties on the normalization of the different signals in each of these categories is parametrized using multinomial probabilities. In particular, based on the $t\bar{t}$ topology, the number of events with one (S_{1b}^k), two (S_{2b}^k), or a different number of b-tagged jets (S_{other}^k) in each bin of $m_{t\bar{t}}$ is expressed as:

$$S_{1b}^k = \mathcal{L}\sigma_{t\bar{t}}^{(\mu_k)} A_{\text{sel}}^k \epsilon_{\text{sel}}^k 2\epsilon_b^k (1 - C_b^k \epsilon_b^k), \quad (3)$$

$$S_{2b}^k = \mathcal{L}\sigma_{t\bar{t}}^{(\mu_k)} A_{\text{sel}}^k \epsilon_{\text{sel}}^k C_b^k (\epsilon_b^k)^2, \quad (4)$$

$$S_{\text{other}}^k = \mathcal{L}\sigma_{t\bar{t}}^{(\mu_k)} A_{\text{sel}}^k \epsilon_{\text{sel}}^k \left[1 - 2\epsilon_b^k (1 - C_b^k \epsilon_b^k) - C_b^k (\epsilon_b^k)^2 \right]. \quad (5)$$

Here, \mathcal{L} is the integrated luminosity, A_{sel}^k is the acceptance of the event selection in the $m_{t\bar{t}}$ bin k , and ϵ_{sel}^k represents the efficiency for an event in the visible phase space to pass the full event selection. The acceptance A_{sel}^k is defined as the fraction of $t\bar{t}$ events in the bin k that, at the generator (particle) level, enter the visible phase space described in Section 3, while ϵ_{sel}^k includes experimental selection criteria, e.g. isolation and trigger requirements. Furthermore, ϵ_b^k represents the b tagging probability and the parameter C_b^k accounts for any residual correlation between the tagging of two b jets in a $t\bar{t}$ event. The quantities A_{sel}^k , ϵ_{sel}^k , ϵ_b^k , and C_b^k are determined from the signal simulation and, although they are not free parameters of the fit, they

vary according to the parameters $\vec{\lambda}$ and m_t^{MC} . In each category, the remaining effects of the systematic uncertainties on signal processes are treated as shape uncertainties. The quantities s_i^k in Eq. 2 are then derived from the signal shape and normalization in the corresponding category. In this way, a precise parametrization of the dependence of signal normalizations on the nuisance parameters and m_t^{MC} is obtained. In fact, the parameters in Eqs. 3–5 are less subject to statistical fluctuations than the s_i^k .

In order to constrain each individual $\sigma_{t\bar{t}}^{(\mu_k)}$, events with at least two jets are further divided into subcategories of $m_{t\bar{t}}^{\text{reco}}$, using the same binning as for $m_{t\bar{t}}$ (Table 1). The choice of the input distributions to the fit in the different event categories is summarized in Table 2. The total number of events is chosen as input to the fit for all subcategories with zero or more than two b-tagged jets, where the contribution of the background processes is the largest, in order to mitigate the sensitivity of the measurement to the shape of the distributions of background processes. The same choice is made for the subcategories corresponding to the last bin in $m_{t\bar{t}}^{\text{reco}}$, where the statistical uncertainty in both data and simulation is large, and for events with less than two jets, where the kinematic reconstruction cannot be performed. In the remaining subcategories with one b-tagged jet, the minimum invariant mass found when combining the reconstructed b jet and a lepton, referred to as the $m_{\ell b}^{\text{min}}$ distribution, is fitted. This distribution provides the sensitivity to constrain m_t^{MC} [49]. In the remaining subcategories with two b-tagged jets, the p_T spectrum of the softest selected jet in the event is used to constrain jet energy scale uncertainties at small values of p_T , the kinematic range where systematic uncertainties are the largest. The distributions used in the fit are compared to the data after the fit in Appendix A.

Table 2: Input distributions to the fit in the different event categories. The number of jets, the number of b-tagged jets, the number of events, and the p_T of the softest jet are denoted with N_{jets} , N_b , N_{events} , and “jet p_T^{min} ”, respectively, while the category corresponding to the bin k in $m_{t\bar{t}}^{\text{reco}}$ is indicated with “ $m_{t\bar{t}}^{\text{reco}} k$ ”.

	$N_b = 1$	$N_b = 2$	Other N_b
$N_{\text{jets}} < 2$	N_{events}	n.a.	N_{events}
$m_{t\bar{t}}^{\text{reco}} 1$	$m_{\ell b}^{\text{min}}$	jet p_T^{min}	N_{events}
$m_{t\bar{t}}^{\text{reco}} 2$	$m_{\ell b}^{\text{min}}$	jet p_T^{min}	N_{events}
$m_{t\bar{t}}^{\text{reco}} 3$	$m_{\ell b}^{\text{min}}$	jet p_T^{min}	N_{events}
$m_{t\bar{t}}^{\text{reco}} 4$	N_{events}	N_{events}	N_{events}

The efficiencies of the kinematic reconstruction in data and simulation have been investigated in Ref. [33] and they were found to differ by 0.2%. Therefore, the efficiency in the simulation is corrected to match the one in data. An uncertainty of 0.2% is assigned to each bin of $m_{t\bar{t}}$ independently. The same uncertainty is also assigned to $t\bar{t}$ events with one or two b-tagged jets, independently. For $t\bar{t}$ events with zero or more than two b-tagged jets, where the combinatorial background is larger, an uncertainty of 0.5% is conservatively assigned. These uncertainties are treated as uncorrelated to account for possible differences between the different $m_{t\bar{t}}$ bins and categories of b-tagged jet multiplicity. Similarly, an additional uncertainty of 1% is assigned to the sum of the background processes, independently for each bin of $m_{t\bar{t}}^{\text{reco}}$, in order to reduce the correlation between the signal and the background templates. The impact of these uncertainties on the final results is found to be small compared to the total uncertainty.

The dependence of the signal shapes, of the parameters A_{sel}^k , ϵ_{sel}^k , ϵ_b^k , and C_b^k , and of the background contributions on m_t^{MC} and on the nuisance parameters $\vec{\lambda}$ is modelled using second-

order polynomials [14]. In the fit, Gaussian priors are assumed for all the nuisance parameters. The negative log-likelihood is then minimized, using the MINUIT program [50], with respect to $\sigma_{\text{t}\bar{\text{t}}}^{(\mu_k)}$, m_{t}^{MC} , and $\vec{\lambda}$. Finally, the fit uncertainties in the various $\sigma_{\text{t}\bar{\text{t}}}^{(\mu_k)}$ are determined using MINOS [50]. Additional extrapolation uncertainties, which reflect the impact of modelling uncertainties on A_{sel}^k , are estimated without taking into account the constraints obtained in the visible phase space [14]. Moreover, an additional uncertainty arising from the limited statistical precision of the simulation is estimated using MC pseudo-experiments [14], where templates are varied within their statistical uncertainties taking into account the correlations between the nominal templates and the templates corresponding to the systematic variations. The template dependencies are then rederived and the fit to the data is repeated more than ten thousand times. For each parameter of interest, the root-mean-square of the best fit values obtained with this procedure is taken as an additional uncertainty and added in quadrature to the total uncertainty from the fit.

The measured $\sigma_{\text{t}\bar{\text{t}}}^{(\mu_k)}$ are shown in Fig. 2 and compared to fixed-order theoretical predictions in the $\overline{\text{MS}}$ scheme at NLO [51] implemented for the purpose of this analysis in the MCFM v6.8 program [52, 53]. In the calculation, the renormalization scale, μ_r , and factorization scale, μ_f , are both set to m_{t} . The $\overline{\text{MS}}$ mass of the top quark evaluated at the scale $\mu = m_{\text{t}}$ is denoted with $m_{\text{t}}(m_{\text{t}})$. The calculation is interfaced with the ABMP16_5_nlo PDF set [54], which is the only available PDF set where m_{t} is treated in the $\overline{\text{MS}}$ scheme and where the correlations between the gluon PDF, α_S , and m_{t} are taken into account. In the calculation, the value of α_S at the Z boson mass, $\alpha_S(m_Z)$, is set to the value determined in the ABMP16_5_nlo fit, which in the central PDF corresponds to 0.1191 [54]. In order to demonstrate the sensitivity to the top quark mass, predictions for $d\sigma_{\text{t}\bar{\text{t}}}/dm_{\text{t}\bar{\text{t}}}$ obtained with different values of $m_{\text{t}}(m_{\text{t}})$ are shown. Furthermore, it is worth noting that this method provides a cross section result with significantly improved precision compared to measurements that perform unfolding as a separate step, e.g. as the one described in Ref. [33].

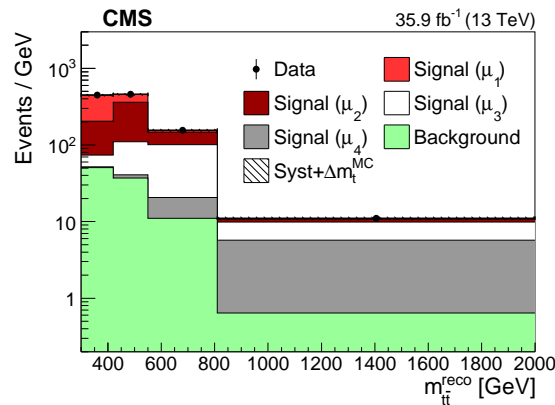


Figure 1: Distribution of $m_{\text{t}\bar{\text{t}}}^{\text{reco}}$ after the fit to the data, with the same binning as used in the fit. The hatched band corresponds to the total uncertainty in the predicted yields, including the contribution from m_{t}^{MC} ($\Delta m_{\text{t}}^{\text{MC}}$) and all correlations. The $\text{t}\bar{\text{t}}$ MC sample is split into four subsamples, denoted with “Signal (μ_k)”, corresponding to bins of $m_{\text{t}\bar{\text{t}}}$ at the parton level. The first and last bins contain all events with $m_{\text{t}\bar{\text{t}}}^{\text{reco}} < 420$ GeV and $m_{\text{t}\bar{\text{t}}}^{\text{reco}} > 810$ GeV, respectively.

The dominant uncertainties in the measured $\sigma_{\text{t}\bar{\text{t}}}^{(\mu_k)}$ are associated with the integrated luminosity, the lepton identification efficiencies, the jet energy scales and, at large $m_{\text{t}\bar{\text{t}}}$, the modelling of the top quark p_{T} . The two latter uncertainties are marginally constrained in the fit, while the first two are not constrained. Furthermore, the post-fit values of all nuisance parameters are found

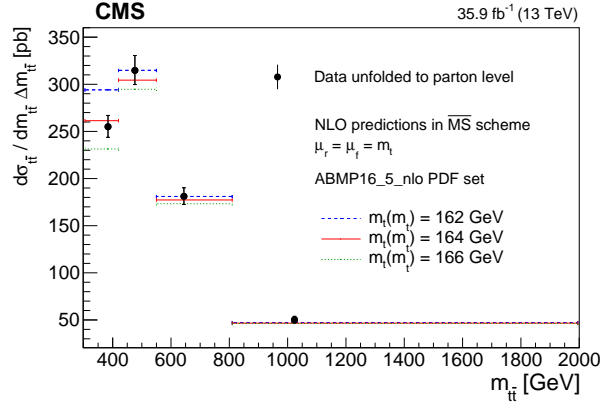


Figure 2: Measured values of $\sigma_{\text{tt}}^{(\mu_k)}$ (markers) and their uncertainties (vertical error bars) compared to NLO predictions in the $\overline{\text{MS}}$ scheme obtained with different values of $m_t(m_t)$ (horizontal lines of different styles). The values of $\sigma_{\text{tt}}^{(\mu_k)}$ are shown at the representative scale of the process μ_k , defined as the centre-of-gravity of bin k in m_{tt} . The first and last bins contain all events with $m_{\text{tt}} < 420$ GeV and $m_{\text{tt}} > 810$ GeV, respectively.

to be compatible with their pre-fit value, within one standard deviation. The numerical values of the measured $\sigma_{\text{tt}}^{(\mu_k)}$, their correlations, the impact of the various sources of uncertainty, and the pulls and constraints of the nuisance parameters related to the modelling uncertainties can be found in Appendix A.

5 Extraction of the running of the top quark mass

The measured differential cross section is used to extract the running of the top quark $\overline{\text{MS}}$ mass at NLO as a function of the scale $\mu = m_{\text{tt}}$. The procedure is similar to the one used to extract the running of the charm quark mass [12]. The value of $m_t(m_t)$ is determined independently in each bin of m_{tt} from a χ^2 fit of fixed-order theoretical predictions at NLO to the measured $\sigma_{\text{tt}}^{(\mu_k)}$. The theoretical predictions are obtained as described in Section 4 for Fig. 2. The χ^2 definition follows the one described in Ref. [55], which accounts for asymmetries in the input uncertainties. The extracted $m_t(m_t)$ are then converted to $m_t(\mu_k)$ using the CRUNDEC v3.0 program [56], where μ_k is the representative scale of the process in a given bin of m_{tt} , as described in Section 3. As relevant in a NLO calculation, the conversion is performed with one-loop precision, assuming five active flavours ($n_f = 5$) and $\alpha_s(m_Z) = 0.1191$ consistently with the used PDF set. This procedure is equivalent to extracting directly $m_t(\mu_k)$ in each bin. Furthermore, the result does not depend on the exact choice of μ_k , provided that it is representative of the physical energy scale of the process. In fact, a change in μ_k would correspond to a change in $m_t(\mu_k)$ according to the RGE. The extracted values of $m_t(\mu_k)$ and their uncertainties can be found in Appendix A.

In order to benefit from the cancellation of correlated uncertainties in the measured $\sigma_{\text{tt}}^{(\mu_k)}$, the ratios of the various $m_t(\mu_k)$ to $m_t(\mu_2)$ are considered. In particular, the quantities $r_{12} = m_t(\mu_1)/m_t(\mu_2)$, $r_{32} = m_t(\mu_3)/m_t(\mu_2)$, and $r_{42} = m_t(\mu_4)/m_t(\mu_2)$ are extracted. With this approach the running of m_t , i.e. the quantity predicted by the RGE (Eq. 1), is accessed directly. The measurement at the scale μ_2 is chosen as a reference in order to minimize the correlation between the extracted ratios.

Four different types of systematic uncertainty are considered for the ratios: the uncertainty in

the various $\sigma_{\text{t}\bar{\text{t}}}^{(\mu_k)}$ in the visible phase space (referred to as fit uncertainty), the extrapolation uncertainties, the uncertainties in the proton PDFs, and the uncertainty in the value of $\alpha_S(m_Z)$. The fit uncertainty includes experimental and modelling uncertainties described in Section 3. Scale variations in the MCFM predictions are not performed, since the scale dependence of m_t is being investigated at a fixed order in perturbation theory. In fact, scale variations in the hard scattering cross section are conventionally performed as a means of estimating the effect of missing higher order corrections and are therefore not applicable in this context.

Uncertainties in the proton PDFs affect the MCFM prediction and therefore the extracted values of the various $m_t(\mu_k)$. In order to estimate their impact, the calculation is repeated for each eigenvector of the PDF set and the differences in the extracted ratios are added in quadrature to yield the total PDF uncertainties. In the ABMP16.5_nlo PDF set, $\alpha_S(m_Z)$ is determined simultaneously with the PDFs, therefore its uncertainty is incorporated in that of the PDFs. However, the uncertainty in $\alpha_S(m_Z)$ also affects the CRUNDEC conversion from $m_t(m_t)$ to $m_t(\mu_k)$. This effect is estimated independently and is found to be negligible.

The impact of extrapolation uncertainties is estimated by varying the measured $\sigma_{\text{t}\bar{\text{t}}}^{(\mu_k)}$ within their extrapolation uncertainty, separately for each source and simultaneously in the different bins in $m_{\text{t}\bar{\text{t}}}$, taking the correlations into account. The various contributions are added in quadrature to yield the total extrapolation uncertainty.

The correlations between the extracted masses arising from the fit uncertainty are estimated using MC pseudo-experiments, taking the correlations between the measured $\sigma_{\text{t}\bar{\text{t}}}^{(\mu_k)}$ as inputs. The uncertainties are then propagated to the ratios using linear uncertainty propagation, taking the estimated correlations into account. The numerical values of the ratios are determined to be:

$$\begin{aligned} r_{12} &= 1.030 \pm 0.018 \text{ (fit)} \begin{matrix} +0.003 \\ -0.006 \end{matrix} \text{ (PDF+}\alpha_S) \begin{matrix} +0.003 \\ -0.002 \end{matrix} \text{ (extr)}, \\ r_{32} &= 0.982 \pm 0.025 \text{ (fit)} \begin{matrix} +0.006 \\ -0.005 \end{matrix} \text{ (PDF+}\alpha_S) \pm 0.004 \text{ (extr)}, \\ r_{42} &= 0.904 \pm 0.050 \text{ (fit)} \begin{matrix} +0.019 \\ -0.017 \end{matrix} \text{ (PDF+}\alpha_S) \begin{matrix} +0.017 \\ -0.013 \end{matrix} \text{ (extr)}. \end{aligned}$$

Here, the fit uncertainty (fit), the combination of PDF and α_S uncertainty (PDF+ α_S), and the extrapolation uncertainty (extr) are given. The most relevant sources of experimental uncertainty are the integrated luminosity, the lepton identification efficiencies, and the jet energy scale and resolution. Among modelling uncertainties related to the POWHEG +PYTHIA 8 simulation of the $\text{t}\bar{\text{t}}$ signal, the largest contributions originate from the scale variations in the parton shower, the uncertainty in the shape of the p_T spectrum of the top quark, and the matching scale between the matrix element and the parton shower. The statistical uncertainties are found to be negligible. The correlations between the ratios arising from the fit uncertainty are investigated using a pseudo-experiment procedure which consists in repeating the extraction of the ratios using pseudo-measurements of $\sigma_{\text{t}\bar{\text{t}}}^{(\mu_k)}$, generated according to the corresponding fitted values, uncertainties, and correlations. With ρ_{ik} being the correlation between r_{i2} and r_{k2} , the results are $\rho_{13} = 13\%$, $\rho_{14} = -45\%$, and $\rho_{34} = 11\%$.

The extracted ratios $m_t(\mu_k)/m_t(\mu_2)$ are shown in Fig. 3 (left) together with the RGE prediction (Eq. 1) at one-loop precision. In the figure, the reference scale μ_2 is indicated with μ_{ref} , and the RGE evolution is calculated from the initial scale $\mu_0 = \mu_{\text{ref}}$. Good agreement between the extracted running and the RGE prediction is observed.

For comparison, the $\overline{\text{MS}}$ mass of the top quark is also extracted from the inclusive cross section measured in Ref. [14], using HATHOR 2.0 [57] predictions at NLO interfaced with the ABMP16.5_nlo PDF set, and is denoted with $m_t^{\text{incl}}(m_t)$. Fig. 3 (right) compares the extracted

ratios $m_t(\mu_k)/m_t(\mu_2)$ to the value of $m_t^{\text{incl}}(m_t)/m_t(\mu_2)$. The uncertainty in $m_t^{\text{incl}}(m_t)$ includes fit, extrapolation, and PDF uncertainties, and is evolved to higher scales, while the value of $m_t(\mu_2)$ in the ratio $m_t^{\text{incl}}(m_t)/m_t(\mu_2)$ is taken without uncertainty. Here, the RGE evolution is calculated from the initial scale $\mu_0 = m_t^{\text{incl}}(m_t)$, which corresponds to about 163 GeV. The extracted value of $m_t^{\text{incl}}(m_t)$ and its uncertainty can be found in Appendix A.

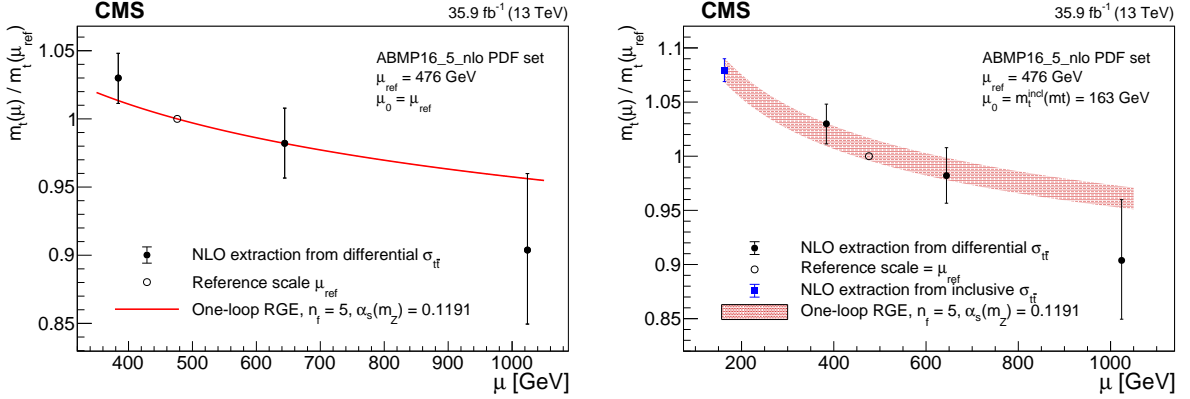


Figure 3: Extracted running of the top quark mass $m_t(\mu)/m_t(\mu_{\text{ref}})$ compared to the RGE prediction at one-loop precision, with $n_f = 5$, evolved from the initial scale $\mu_0 = \mu_{\text{ref}} = 476$ GeV (left). The result is compared to the value of $m_t^{\text{incl}}(m_t)/m_t(\mu_{\text{ref}})$, where $m_t^{\text{incl}}(m_t)$ is the value of $m_t(m_t)$ extracted from the inclusive cross section measured in Ref. [14], which is based on the same data set. The uncertainty in $m_t^{\text{incl}}(m_t)$ is evolved from the initial scale $\mu_0 = m_t^{\text{incl}}(m_t)$, which corresponds to about 163 GeV, using the same RGE prediction (right).

Finally, the extracted running is parametrized with the function

$$f(x, \mu) = x [r(\mu) - 1] + 1, \quad (6)$$

where $r(\mu) = m_t(\mu)/m_t(\mu_2)$ corresponds to the RGE prediction shown in Fig. 3 (left). In particular, $f(x, \mu)$ corresponds to $r(\mu)$ for $x = 1$ and to 1, i.e. no running, for $x = 0$. The best fit value for x , denoted with \hat{x} , is determined via a χ^2 fit to the extracted ratios taking the correlations ρ_{ik} into account, and is found to be

$$\hat{x} = 2.05 \pm 0.61 \text{ (fit)} \begin{matrix} +0.31 \\ -0.55 \end{matrix} \text{ (PDF + } \alpha_s) \begin{matrix} +0.24 \\ -0.49 \end{matrix} \text{ (extr).}$$

The result shows agreement between the extracted running and the RGE prediction at one-loop precision within 1.1 standard deviations in the Gaussian approximation and excludes the no-running hypothesis at above 95% confidence level (2.1 standard deviations) in the same approximation.

6 Summary

In this Letter, the first experimental investigation of the running of the top quark mass, m_t , is presented. The running is extracted from a measurement of the differential top quark-antiquark ($t\bar{t}$) cross section as a function of the invariant mass of the $t\bar{t}$ system, $m_{t\bar{t}}$. The differential $t\bar{t}$ cross section, $d\sigma_{t\bar{t}}/dm_{t\bar{t}}$, is determined at the parton level using a maximum-likelihood fit to distributions of final-state observables, using $t\bar{t}$ candidate events in the $e^\pm\mu^\mp$ channel. This technique allows the nuisance parameters to be constrained simultaneously with the differential cross section in the visible phase space and therefore provides results with significantly

improved precision compared to conventional procedures in which the unfolding is performed as a separate step. The analysis is performed using proton-proton collision data at a centre-of-mass energy of 13 TeV recorded by the CMS detector at the CERN LHC in 2016, corresponding to an integrated luminosity of 35.9 fb^{-1} .

The running mass $m_t(\mu)$, as defined in the modified minimal subtraction ($\overline{\text{MS}}$) renormalization scheme, is extracted at one-loop precision as a function of $m_{\text{t}\bar{\text{t}}}$ by comparing fixed-order theoretical predictions at next-to-leading order to the measured $d\sigma_{\text{t}\bar{\text{t}}}/dm_{\text{t}\bar{\text{t}}}$. The extracted running of m_t is found to be in agreement with the prediction of the corresponding renormalization group equation, within 1.1 standard deviations, and the no-running hypothesis is excluded at above 95% confidence level. The running of m_t is probed up to a scale of the order of 1 TeV.

Acknowledgments

We congratulate our colleagues in the CERN accelerator departments for the excellent performance of the LHC and thank the technical and administrative staffs at CERN and at other CMS institutes for their contributions to the success of the CMS effort. In addition, we gratefully acknowledge the computing centres and personnel of the Worldwide LHC Computing Grid for delivering so effectively the computing infrastructure essential to our analyses. Finally, we acknowledge the enduring support for the construction and operation of the LHC and the CMS detector provided by the following funding agencies: BMBWF and FWF (Austria); FNRS and FWO (Belgium); CNPq, CAPES, FAPERJ, FAPERGS, and FAPESP (Brazil); MES (Bulgaria); CERN; CAS, MoST, and NSFC (China); COLCIENCIAS (Colombia); MSES and CSF (Croatia); RPF (Cyprus); SENESCYT (Ecuador); MoER, ERC IUT, PUT and ERDF (Estonia); Academy of Finland, MEC, and HIP (Finland); CEA and CNRS/IN2P3 (France); BMBF, DFG, and HGF (Germany); GSRT (Greece); NKFI (Hungary); DAE and DST (India); IPM (Iran); SFI (Ireland); INFN (Italy); MSIP and NRF (Republic of Korea); MES (Latvia); LAS (Lithuania); MOE and UM (Malaysia); BUAP, CINVESTAV, CONACYT, LNS, SEP, and UASLP-FAI (Mexico); MOS (Montenegro); MBIE (New Zealand); PAEC (Pakistan); MSHE and NSC (Poland); FCT (Portugal); JINR (Dubna); MON, RosAtom, RAS, RFBR, and NRC KI (Russia); MESTD (Serbia); SEIDI, CPAN, PCTI, and FEDER (Spain); MOSTR (Sri Lanka); Swiss Funding Agencies (Switzerland); MST (Taipei); ThEPCenter, IPST, STAR, and NSTDA (Thailand); TUBITAK and TAEK (Turkey); NASU and SFFR (Ukraine); STFC (United Kingdom); DOE and NSF (USA).

Individuals have received support from the Marie-Curie programme and the European Research Council and Horizon 2020 Grant, contract Nos. 675440, 752730, and 765710 (European Union); the Leventis Foundation; the A.P. Sloan Foundation; the Alexander von Humboldt Foundation; the Belgian Federal Science Policy Office; the Fonds pour la Formation à la Recherche dans l'Industrie et dans l'Agriculture (FRIA-Belgium); the Agentschap voor Innovatie door Wetenschap en Technologie (IWT-Belgium); the F.R.S.-FNRS and FWO (Belgium) under the "Excellence of Science – EOS" – be.h project n. 30820817; the Beijing Municipal Science & Technology Commission, No. Z181100004218003; the Ministry of Education, Youth and Sports (MEYS) of the Czech Republic; the Lendület ("Momentum") Programme and the János Bolyai Research Scholarship of the Hungarian Academy of Sciences, the New National Excellence Program ÚNKP, the NKFI research grants 123842, 123959, 124845, 124850, 125105, 128713, 128786, and 129058 (Hungary); the Council of Science and Industrial Research, India; the HOMING PLUS programme of the Foundation for Polish Science, cofinanced from European Union, Regional Development Fund, the Mobility Plus programme of the Ministry of Science and Higher Education, the National Science Center (Poland), contracts Harmonia 2014/14/M/ST2/00428, Opus 2014/13/B/ST2/02543, 2014/15/B/ST2/03998, and 2015/19/B/ST2/02861, Sonata-bis

2012/07/E/ST2/01406; the National Priorities Research Program by Qatar National Research Fund; the Ministry of Science and Education, grant no. 3.2989.2017 (Russia); the Programa Estatal de Fomento de la Investigación Científica y Técnica de Excelencia María de Maeztu, grant MDM-2015-0509 and the Programa Severo Ochoa del Principado de Asturias; the Thalís and Aristeia programmes cofinanced by EU-ESF and the Greek NSRF; the Rachadapisek Sompot Fund for Postdoctoral Fellowship, Chulalongkorn University and the Chulalongkorn Academic into Its 2nd Century Project Advancement Project (Thailand); the Nvidia Corporation; the Welch Foundation, contract C-1845; and the Weston Havens Foundation (USA).

References

- [1] A. Deur, S. J. Brodsky, and G. F. de Teramond, “The QCD running coupling”, *Prog. Part. Nucl. Phys.* **90** (2016) 1, doi:10.1016/j.pnpnp.2016.04.003, arXiv:1604.08082.
- [2] CMS Collaboration, “Measurement and QCD analysis of double-differential inclusive jet cross sections in pp collisions at $\sqrt{s} = 8$ TeV and cross section ratios to 2.76 and 7 TeV”, *JHEP* **03** (2017) 156, doi:10.1007/JHEP03(2017)156, arXiv:1609.05331.
- [3] P. A. Baikov, K. G. Chetyrkin, and J. H. Kühn, “Quark mass and field anomalous dimensions to $\mathcal{O}(\alpha_S^5)$ ”, *JHEP* **10** (2014) 076, doi:10.1007/JHEP10(2014)076, arXiv:1402.6611.
- [4] T. Luthe, A. Maier, P. Marquard, and Y. Schröder, “Five-loop quark mass and field anomalous dimensions for a general gauge group”, *JHEP* **01** (2017) 081, doi:10.1007/JHEP01(2017)081, arXiv:1612.05512.
- [5] O. Behnke, A. Geiser, and M. Lisovsky, “Charm, beauty and top at HERA”, *Prog. Part. Nucl. Phys.* **84** (2015) 1, doi:10.1016/j.pnpnp.2015.06.002, arXiv:1506.07519.
- [6] DELPHI Collaboration, “Study of b-quark mass effects in multijet topologies with the DELPHI detector at LEP”, *Eur. Phys. J. C* **55** (2008) 525, doi:10.1140/epjc/s10052-008-0631-5, arXiv:0804.3883.
- [7] DELPHI Collaboration, “Determination of the b quark mass at the M_Z scale with the DELPHI detector at LEP”, *Eur. Phys. J. C* **46** (2006) 569, doi:10.1140/epjc/s2006-02497-6.
- [8] ALEPH Collaboration, “A Measurement of the b quark mass from hadronic Z decays”, *Eur. Phys. J. C* **18** (2000) 1, doi:10.1007/s100520000533, arXiv:hep-ex/0008013.
- [9] OPAL Collaboration, “Determination of the b quark mass at the Z mass scale”, *Eur. Phys. J. C* **21** (2001) 411, doi:10.1007/s100520100746, arXiv:hep-ex/0105046.
- [10] A. Brandenburg et al., “Measurement of the running b quark mass using $e^+e^- \rightarrow b\bar{b}g$ events”, *Phys. Lett. B* **468** (1999) 168, doi:10.1016/S0370-2693(99)01194-6, arXiv:hep-ph/9905495.
- [11] ZEUS Collaboration, “Measurement of beauty and charm production in deep inelastic scattering at HERA and measurement of the beauty-quark mass”, *JHEP* **09** (2014) 127, doi:10.1007/JHEP09(2014)127, arXiv:1405.6915.
- [12] A. Gizhko et al., “Running of the charm-quark mass from HERA deep-inelastic scattering data”, *Phys. Lett. B* **775** (2017) 233, doi:10.1016/j.physletb.2017.11.002, arXiv:1705.08863.

-
- [13] L. Mihaila, “Precision calculations in supersymmetric theories”, *Adv. High Energy Phys.* **2013** (2013) 607807, doi:10.1155/2013/607807, arXiv:1310.6178.
- [14] CMS Collaboration, “Measurement of the $t\bar{t}$ production cross section, the top quark mass, and the strong coupling constant using dilepton events in pp collisions at $\sqrt{s} = 13$ TeV”, *Eur. Phys. J. C* **79** (2019) 368, doi:10.1140/epjc/s10052-019-6863-8, arXiv:1812.10505.
- [15] CMS Collaboration, “The CMS trigger system”, *JINST* **12** (2017) P01020, doi:10.1088/1748-0221/12/01/P01020, arXiv:1609.02366.
- [16] CMS Collaboration, “The CMS experiment at the CERN LHC”, *JINST* **3** (2008) S08004, doi:10.1088/1748-0221/3/08/S08004.
- [17] CMS Collaboration, “Particle-flow reconstruction and global event description with the CMS detector”, *JINST* **12** (2017) P10003, doi:10.1088/1748-0221/12/10/P10003, arXiv:1706.04965.
- [18] CMS Collaboration, “Performance of electron reconstruction and selection with the CMS detector in proton-proton collisions at $\sqrt{s} = 8$ TeV”, *JINST* **10** (2015) P06005, doi:10.1088/1748-0221/10/06/P06005, arXiv:1502.02701.
- [19] CMS Collaboration, “Performance of the CMS muon detector and muon reconstruction with proton-proton collisions at $\sqrt{s} = 13$ TeV”, *JINST* **13** (2018) P06015, doi:10.1088/1748-0221/13/06/P06015, arXiv:1804.04528.
- [20] M. Cacciari, G. P. Salam, and G. Soyez, “The anti- k_T jet clustering algorithm”, *JHEP* **04** (2008) 063, doi:10.1088/1126-6708/2008/04/063, arXiv:0802.1189.
- [21] M. Cacciari, G. P. Salam, and G. Soyez, “FastJet user manual”, *Eur. Phys. J. C* **72** (2012) 1896, doi:10.1140/epjc/s10052-012-1896-2, arXiv:1111.6097.
- [22] CMS Collaboration, “Identification of heavy-flavour jets with the CMS detector in pp collisions at 13 TeV”, *JINST* **13** (2018) P05011, doi:10.1088/1748-0221/13/05/P05011, arXiv:1712.07158.
- [23] P. Nason, “A new method for combining NLO QCD with shower Monte Carlo algorithms”, *JHEP* **11** (2004) 040, doi:10.1088/1126-6708/2004/11/040, arXiv:hep-ph/0409146.
- [24] S. Frixione, P. Nason, and C. Oleari, “Matching NLO QCD computations with parton shower simulations: the POWHEG method”, *JHEP* **11** (2007) 070, doi:10.1088/1126-6708/2007/11/070, arXiv:0709.2092.
- [25] S. Alioli, P. Nason, C. Oleari, and E. Re, “A general framework for implementing NLO calculations in shower Monte Carlo programs: the POWHEG BOX”, *JHEP* **06** (2010) 043, doi:10.1007/JHEP06(2010)043, arXiv:1002.2581.
- [26] S. Frixione, P. Nason, and G. Ridolfi, “A positive-weight next-to-leading-order Monte Carlo for heavy flavour hadroproduction”, *JHEP* **09** (2007) 126, doi:10.1088/1126-6708/2007/09/126, arXiv:0707.3088.
- [27] E. Re, “Single-top Wt -channel production matched with parton showers using the POWHEG method”, *Eur. Phys. J. C* **71** (2011) 1547, doi:10.1140/epjc/s10052-011-1547-z, arXiv:1009.2450.

- [28] S. Alioli, P. Nason, C. Oleari, and E. Re, “Vector boson plus one jet production in POWHEG”, *JHEP* **01** (2011) 095, doi:10.1007/JHEP01(2011)095, arXiv:1009.5594.
- [29] T. Sjöstrand et al., “An introduction to PYTHIA 8.2”, *Comput. Phys. Commun.* **191** (2015) 159, doi:10.1016/j.cpc.2015.01.024, arXiv:1410.3012.
- [30] CMS Collaboration, “Investigations of the impact of the parton shower tuning in PYTHIA 8 in the modelling of $t\bar{t}$ at $\sqrt{s} = 8$ and 13 TeV”, CMS Physics Analysis Summary CMS-PAS-TOP-16-021, 2016.
- [31] P. Skands, S. Carrazza, and J. Rojo, “Tuning PYTHIA 8.1: the Monash 2013 tune”, *Eur. Phys. J. C* **74** (2014) 3024, doi:10.1140/epjc/s10052-014-3024-y, arXiv:1404.5630.
- [32] NNPDF Collaboration, “Parton distributions for the LHC Run II”, *JHEP* **04** (2015) 040, doi:10.1007/JHEP04(2015)040, arXiv:1410.8849.
- [33] CMS Collaboration, “Measurements of $t\bar{t}$ differential cross sections in proton-proton collisions at $\sqrt{s} = 13$ TeV using events containing two leptons”, *JHEP* **02** (2019) 149, doi:10.1007/JHEP02(2019)149, arXiv:1811.06625.
- [34] CMS Collaboration, “Jet energy scale and resolution in the CMS experiment in pp collisions at 8 TeV”, *JINST* **12** (2017) P02014, doi:10.1088/1748-0221/12/02/P02014, arXiv:1607.03663.
- [35] CMS Collaboration, “Jet algorithms performance in 13 TeV data”, CMS Physics Analysis Summary CMS-PAS-JME-16-003, 2017.
- [36] CMS Collaboration, “CMS luminosity measurements for the 2016 data taking period”, CMS Physics Analysis Summary CMS-PAS-LUM-17-001, 2017.
- [37] M. Cacciari et al., “The $t\bar{t}$ cross-section at 1.8 TeV and 1.96 TeV: a study of the systematics due to parton densities and scale dependence”, *JHEP* **04** (2004) 068, doi:10.1088/1126-6708/2004/04/068, arXiv:hep-ph/0303085.
- [38] S. Catani, D. de Florian, M. Grazzini, and P. Nason, “Soft gluon resummation for Higgs boson production at hadron colliders”, *JHEP* **07** (2003) 028, doi:10.1088/1126-6708/2003/07/028, arXiv:hep-ph/0306211.
- [39] S. Dulat et al., “New parton distribution functions from a global analysis of quantum chromodynamics”, *Phys. Rev. D* **93** (2016) 033006, doi:10.1103/PhysRevD.93.033006, arXiv:1506.07443.
- [40] M. G. Bowler, “ e^+e^- production of heavy quarks in the string model”, *Z. Phys. C* **11** (1981) 169, doi:10.1007/BF01574001.
- [41] C. Peterson, D. Schlatter, I. Schmitt, and P. M. Zerwas, “Scaling violations in inclusive e^+e^- annihilation spectra”, *Phys. Rev. D* **27** (1983) 105, doi:10.1103/PhysRevD.27.105.
- [42] S. Argyropoulos and T. Sjöstrand, “Effects of color reconnection on $t\bar{t}$ final states at the LHC”, *JHEP* **11** (2014) 043, doi:10.1007/JHEP11(2014)043, arXiv:1407.6653.

-
- [43] J. R. Christiansen and P. Z. Skands, “String formation beyond leading colour”, *JHEP* **08** (2015) 003, doi:10.1007/JHEP08(2015)003, arXiv:1505.01681.
- [44] CMS Collaboration, “Measurement of the top quark Yukawa coupling from $t\bar{t}$ kinematic distributions in the lepton+jets final state in proton-proton collisions at $\sqrt{s} = 13$ TeV”, *Phys. Rev. D* **100** (2019) 072007, doi:10.1103/PhysRevD.100.072007, arXiv:1907.01590.
- [45] CMS Collaboration, “Measurement of the top quark polarization and $t\bar{t}$ spin correlations using dilepton final states in proton-proton collisions at $\sqrt{s} = 13$ TeV”, *Phys. Rev. D* **100** (2019) 072002, doi:10.1103/PhysRevD.100.072002, arXiv:1907.03729.
- [46] CMS Collaboration, “Measurement of normalized differential $t\bar{t}$ cross sections in the dilepton channel from pp collisions at $\sqrt{s} = 13$ TeV”, *JHEP* **04** (2018) 060, doi:10.1007/JHEP04(2018)060, arXiv:1708.07638.
- [47] CMS Collaboration, “Measurement of differential cross sections for top quark pair production using the lepton+jets final state in proton-proton collisions at 13 TeV”, *Phys. Rev. D* **95** (2017) 092001, doi:10.1103/PhysRevD.95.092001, arXiv:1610.04191.
- [48] CMS Collaboration, “Measurement of inclusive and differential Higgs boson production cross sections in the diphoton decay channel in proton-proton collisions at $\sqrt{s} = 13$ TeV”, *JHEP* **01** (2019) 183, doi:10.1007/JHEP01(2019)183, arXiv:1807.03825.
- [49] S. Biswas, K. Melnikov, and M. Schulze, “Next-to-leading order QCD effects and the top quark mass measurements at the LHC”, *JHEP* **08** (2010) 048, doi:10.1007/JHEP08(2010)048, arXiv:1006.0910.
- [50] F. James and M. Roos, “MINUIT: a system for function minimization and analysis of the parameter errors and correlations”, *Comput. Phys. Commun.* **10** (1975) 343, doi:10.1016/0010-4655(75)90039-9.
- [51] M. Dowling and S.-O. Moch, “Differential distributions for top-quark hadro-production with a running mass”, *Eur. Phys. J. C* **74** (2014) 3167, doi:10.1140/epjc/s10052-014-3167-x, arXiv:1305.6422.
- [52] J. M. Campbell and R. K. Ellis, “MCFM for the Tevatron and the LHC”, *Nucl. Phys. B Proc. Suppl.* **205-206** (2010) 10, doi:10.1016/j.nuclphysbps.2010.08.011, arXiv:1007.3492.
- [53] J. M. Campbell and R. K. Ellis, “Top-quark processes at NLO in production and decay”, *J. Phys. G* **42** (2015) 015005, doi:10.1088/0954-3899/42/1/015005, arXiv:1204.1513.
- [54] S. Alekhin, J. Blümlein, and S. Moch, “NLO PDFs from the ABMP16 fit”, *Eur. Phys. J. C* **78** (2018) 477, doi:10.1140/epjc/s10052-018-5947-1, arXiv:1803.07537.
- [55] R. Barlow, “Asymmetric errors”, in *Statistical problems in particle physics, astrophysics and cosmology. Proceedings, Conference, PHYSTAT 2003*, p. WEMT002. Stanford, USA, September, 2003. arXiv:physics/0401042. eConf C030908.
- [56] B. Schmidt and M. Steinhauser, “CRUNDEC: a C++ package for running and decoupling of the strong coupling and quark masses”, *Comput. Phys. Commun.* **183** (2012) 1845, doi:10.1016/j.cpc.2012.03.023, arXiv:1201.6149.

-
- [57] M. Aliev et al., “HATHOR: HAdronic Top and Heavy quarks crOss section calculatoR”, *Comput. Phys. Commun.* **182** (2011) 1034, doi:10.1016/j.cpc.2010.12.040, arXiv:1007.1327.

A Supplemental information

Additional information that complements the content of the Letter is provided. Several acronyms are used. These are: matrix element (ME), final state radiation (FSR), initial state radiation (ISR), parton shower (PS), colour reconnection (CR), early resonance decay (ERD), underlying event (UE), branching fraction (BF), and identification (ID).

The distributions used in the fit are compared to the data after the fit in Figure A.1, and the normalized fit pulls and constraints on the nuisance parameters related to the modelling uncertainties are shown in Figure A.2. By means of the likelihood fit, the quantities $\sigma_{t\bar{t}}^{(\mu_k)}$ are determined to be:

$$\begin{aligned}\sigma_{t\bar{t}}^{(\mu_1)} &= 255 \pm 11 \text{ (syst)} \pm 2 \text{ (stat)} \text{ pb}, \\ \sigma_{t\bar{t}}^{(\mu_2)} &= 315 \pm 15 \text{ (syst)} \pm 2 \text{ (stat)} \text{ pb}, \\ \sigma_{t\bar{t}}^{(\mu_3)} &= 181 \pm 9 \text{ (syst)} \pm 1 \text{ (stat)} \text{ pb}, \\ \sigma_{t\bar{t}}^{(\mu_4)} &= 50 \pm 3 \text{ (syst)} \pm 1 \text{ (stat)} \text{ pb}.\end{aligned}$$

The correlations between the measured $\sigma_{t\bar{t}}^{(\mu_k)}$ are given in Table A.1, while the contribution of the various sources of systematic uncertainties to the total uncertainty can be found in Tables A.2 to A.5. Finally, the extracted values of $m_t(\mu_k)$ are shown in Figure A.3, together with the value of $m_t(m_t)$ extracted from the inclusive $t\bar{t}$ cross section, as described in the Letter. The numerical values of the extracted masses are:

$$\begin{aligned}m_t(\mu_1) &= 155.4 \pm 0.8 \text{ (fit)} \pm 0.2 \text{ (PDF}+\alpha_S) \pm 0.1 \text{ (extr)}^{+0.9}_{-0.6} \text{ (scale)}, \\ m_t(\mu_2) &= 150.9 \pm 3.0 \text{ (fit)}^{+1.1}_{-0.7} \text{ (PDF}+\alpha_S)^{+0.4}_{-0.5} \text{ (extr)}^{+3.9}_{-4.3} \text{ (scale)}, \\ m_t(\mu_3) &= 148.2 \pm 4.6 \text{ (fit)}^{+2.0}_{-1.4} \text{ (PDF}+\alpha_S)^{+0.9}_{-1.0} \text{ (extr)}^{+7.3}_{-9.5} \text{ (scale)}, \\ m_t(\mu_4) &= 136.4 \pm 9.0 \text{ (fit)}^{+3.8}_{-3.0} \text{ (PDF}+\alpha_S)^{+2.8}_{-2.3} \text{ (extr)}^{+9.6}_{-16.1} \text{ (scale)}.\end{aligned}$$

The scale uncertainties are obtained by varying the renormalization and factorization scales by a factor of two, avoiding cases in which $\mu_r/\mu_f = 1/4$ or 4. The total scale uncertainty is then defined as the envelope of the individual variations. Similarly, the value $m_t(m_t)$ determined from the inclusive cross section is:

$$m_t(m_t) = 162.9 \pm 1.6 \text{ (fit+extr+PDF}+\alpha_S)^{+2.5}_{-3.0} \text{ (scale)}.$$

As explained in the Letter, scale uncertainties are not considered in the extraction of the running, which is investigated at a fixed order in perturbation theory.

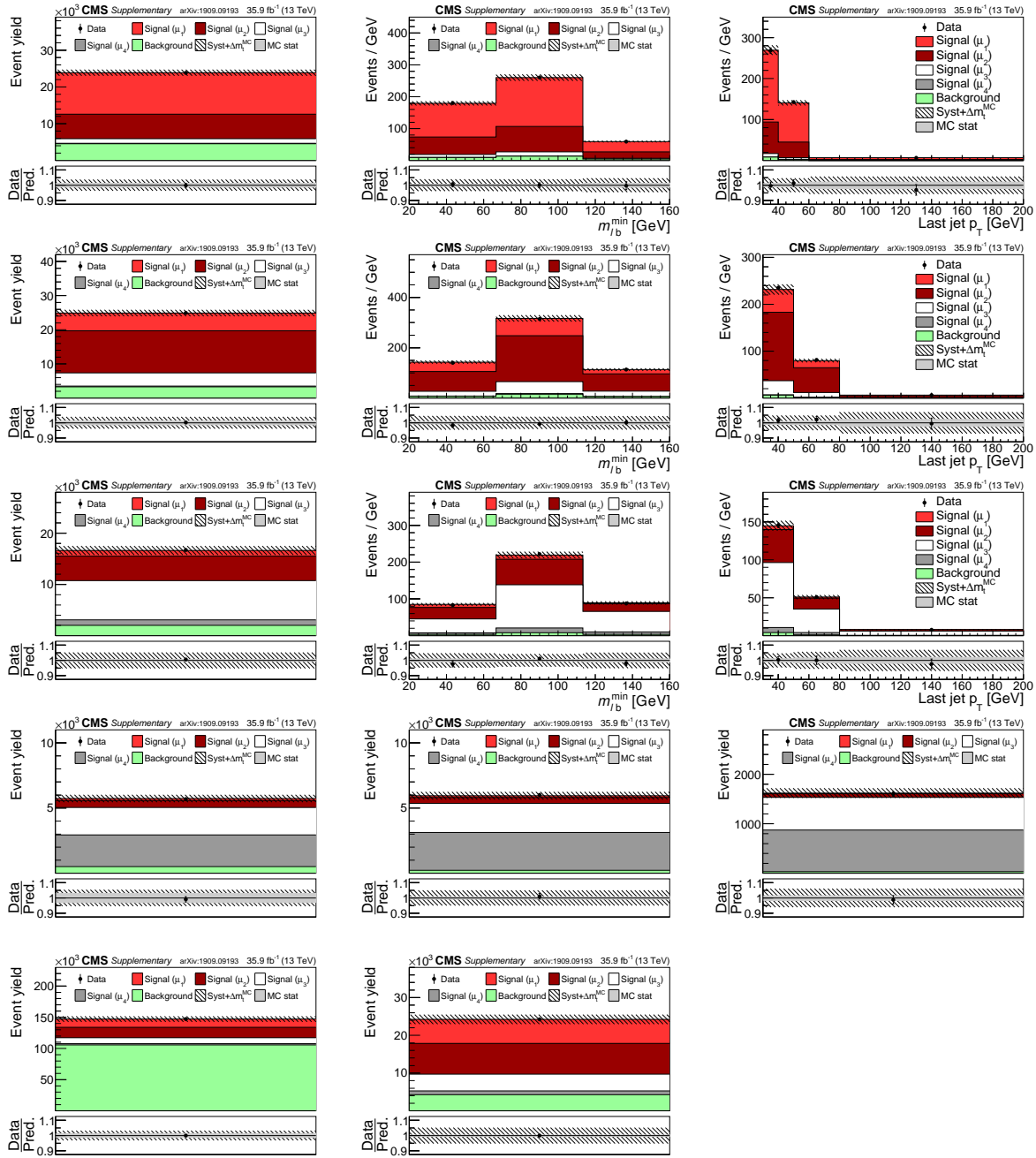


Figure A.1: Comparison between data (points) and post-fit distributions of the expected signal and backgrounds from simulation (shaded histograms) used in the fit of $d\sigma_{t\bar{t}}/dm_{t\bar{t}}$. In the left column events with zero or three or more b-tagged jets are shown. The middle (right) column shows events with exactly one (two) b-tagged jets. Events in the first, second, third, and fourth bin of $m_{t\bar{t}}^{\text{reco}}$ are shown in the first, second, third, and fourth row, respectively, while events with less than two jets are shown in the fifth row. The hatched bands correspond to the total uncertainty in the sum of the predicted yields and include the contribution from the top quark mass (Δm_t^{MC}). The ratios of data to the sum of the predicted yields are shown in the lower panel of each figure. Here, the solid gray band represents the contribution of the statistical uncertainty.

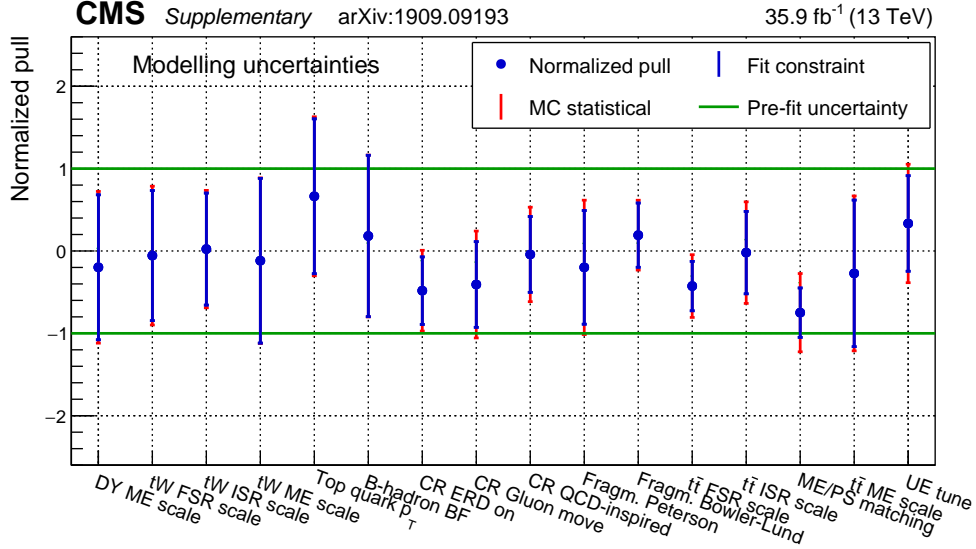


Figure A.2: Pulls and constraints of the nuisance parameters related to the modelling uncertainties. The pulls, defined as the difference between the post-fit and pre-fit values of a nuisance parameter in units of the corresponding pre-fit uncertainty, are represented by the markers, while the constraints, defined as the ratio between the post-fit and pre-fit uncertainties on a nuisance parameter, correspond to the inner vertical bands. The horizontal lines represent the pre-fit uncertainty, and the outer vertical bands indicate the additional uncertainty due to the limited statistics in the simulation, as determined using pseudo-experiments.

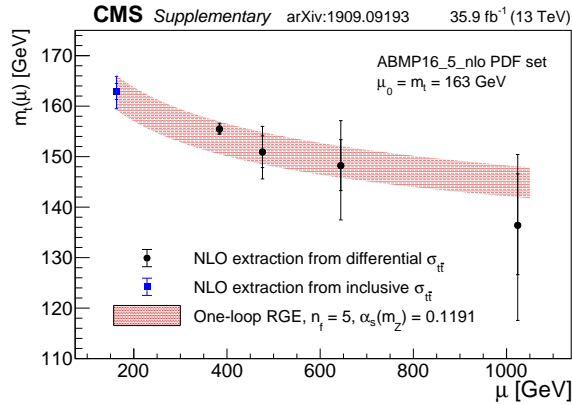


Figure A.3: Values of $m_t(\mu_k)$ extracted from the measured $d\sigma_{t\bar{t}}/dm_{t\bar{t}}$ (round markers), compared to the value of $m_t(m_t)$ extracted from the inclusive $\sigma_{t\bar{t}}$ (square marker). The inner vertical bands correspond to the combination of fit, extrapolation, and PDF uncertainties, while the outer vertical bands include the contribution of the scale uncertainties.

Table A.1: Correlations between the measured $\sigma_{\text{t}\bar{\text{t}}}^{(\mu_k)}$, including all systematic uncertainties.

	$\sigma_{\text{t}\bar{\text{t}}}^{(\mu_1)}$	$\sigma_{\text{t}\bar{\text{t}}}^{(\mu_2)}$	$\sigma_{\text{t}\bar{\text{t}}}^{(\mu_3)}$	$\sigma_{\text{t}\bar{\text{t}}}^{(\mu_4)}$
$\sigma_{\text{t}\bar{\text{t}}}^{(\mu_1)}$	1.00			
$\sigma_{\text{t}\bar{\text{t}}}^{(\mu_2)}$	0.64	1.00		
$\sigma_{\text{t}\bar{\text{t}}}^{(\mu_3)}$	0.72	0.60	1.00	
$\sigma_{\text{t}\bar{\text{t}}}^{(\mu_4)}$	0.32	0.65	0.47	1.00

Table A.2: The relative uncertainty in $\sigma_{t\bar{t}}^{(\mu_k)}$ and its sources, as obtained from the likelihood fit. The MC statistical uncertainty is determined separately, using pseudo-experiments. The individual uncertainties are given without their correlations, which are however accounted for in the total uncertainty. For extrapolation uncertainties, the \pm notation is used if a positive variation produces an increase in $\sigma_{t\bar{t}}^{(\mu_k)}$, while the \mp notation is used otherwise.

Source	Uncertainty [%]
Jet energy scale	1.0
PDF	1.1
Lepton ID/isolation	2.2
Electron energy	0.5
b quark fragmentation	1.1
b tagging	0.2
Colour reconnection	0.7
Kinematic reconstruction	0.4
DY ME scale	0.4
Jet energy resolution	0.2
Muon energy scale	0.1
Pile-up	0.5
tW FSR scale	0.2
tW ISR scale	0.2
tW ME scale	0.2
m_t^{MC}	0.5
Top quark p_T	0.7
Trigger	0.3
b hadron BF	0.1
$t\bar{t}$ FSR scale	0.7
$t\bar{t}$ ISR scale	0.3
ME/PS matching	0.2
$t\bar{t}$ ME scale	0.3
UE tune	0.3
DY background	0.9
tW background	0.6
W+jets background	0.1
Diboson background	0.6
$t\bar{t}$ background	0.3
Integrated luminosity	2.6
Statistical	0.7
MC statistical	1.5
Extrapolation uncertainties	
$t\bar{t}$ ISR scale	± 0.2
$t\bar{t}$ FSR scale	± 0.1
$t\bar{t}$ ME scale	± 0.1
UE tune	$\mp_{0.1}^{<0.1}$
PDF	$\pm_{0.5}^{0.8}$
Top quark p_T	$\pm_{0.1}^{<0.1}$
Total $\sigma_{t\bar{t}}^{(\mu_1)}$ uncertainty	$+4.7$ -4.4

Table A.3: Same as Table A.2, but for $\sigma_{\text{t}\bar{\text{t}}}^{(\mu_2)}$.

Source	Uncertainty [%]
Jet energy scale	1.3
PDF	1.0
Lepton ID/isolation	2.3
Electron energy	0.4
b quark fragmentation	1.0
b tagging	0.5
Colour reconnection	1.0
Kinematic reconstruction	0.4
DY ME scale	0.2
Jet energy resolution	0.5
Muon energy scale	0.2
Pile-up	0.2
tW FSR scale	0.2
tW ISR scale	0.2
tW ME scale	0.2
m_{t}^{MC}	0.4
Top quark p_{T}	0.4
Trigger	0.4
b hadron BF	0.2
$\text{t}\bar{\text{t}}$ FSR scale	1.5
$\text{t}\bar{\text{t}}$ ISR scale	0.3
ME/PS matching	0.8
$\text{t}\bar{\text{t}}$ ME scale	0.8
UE tune	0.2
DY background	1.2
tW background	1.1
W+jets background	0.2
Diboson background	0.3
$\text{t}\bar{\text{t}}$ background	0.2
Integrated luminosity	2.6
Statistical	0.6
MC statistical	1.8
Extrapolation uncertainties	
$\text{t}\bar{\text{t}}$ ISR scale	$\mp_{0.1}^{0.2}$
$\text{t}\bar{\text{t}}$ FSR scale	$\mp_{0.1}^{<0.1}$
$\text{t}\bar{\text{t}}$ ME scale	$\mp_{0.2}^{0.1}$
UE tune	$\mp_{<0.1}^{0.1}$
PDF	$\pm_{0.6}^{0.8}$
Top quark p_{T}	± 0.1
Total $\sigma_{\text{t}\bar{\text{t}}}^{(\mu_2)}$ uncertainty	$+5.0$ -4.8

Table A.4: Same as Table A.2, but for $\sigma_{\text{t}\bar{\text{t}}}^{(\mu_3)}$.

Source	Uncertainty [%]
Jet energy scale	1.8
PDF	1.2
Lepton ID/isolation	2.2
Electron energy	0.5
b quark fragmentation	1.1
b tagging	0.7
Colour reconnection	0.7
Kinematic reconstruction	0.3
DY ME scale	0.1
Jet energy resolution	0.1
Muon energy scale	0.1
Pile-up	0.3
tW FSR scale	0.1
tW ISR scale	0.1
tW ME scale	0.1
m_{t}^{MC}	0.6
Top quark p_{T}	1.2
Trigger	0.4
b hadron BF	0.1
$\text{t}\bar{\text{t}}$ FSR scale	0.5
$\text{t}\bar{\text{t}}$ ISR scale	0.5
ME/PS matching	0.5
$\text{t}\bar{\text{t}}$ ME scale	0.7
UE tune	0.2
DY background	1.2
tW background	0.9
W+jets background	0.1
Diboson background	0.3
$\text{t}\bar{\text{t}}$ background	0.1
Integrated luminosity	2.6
Statistical	0.8
MC statistical	1.4
Extrapolation uncertainties	
$\text{t}\bar{\text{t}}$ ISR scale	$\pm_{0.1}^{0.2}$
$\text{t}\bar{\text{t}}$ FSR scale	$\pm_{<0.1}^{0.2}$
$\text{t}\bar{\text{t}}$ ME scale	$\mp_{0.5}^{0.4}$
UE tune	± 0.1
PDF	$\pm_{0.6}^{0.9}$
Top quark p_{T}	$\pm_{0.4}^{0.2}$
Total $\sigma_{\text{t}\bar{\text{t}}}^{(\mu_3)}$ uncertainty	$+5.0$ -4.8

Table A.5: Same as Table A.2, but for $\sigma_{\text{t}\bar{\text{t}}}^{(\mu_4)}$.

Source	Uncertainty [%]
Jet energy scale	2.2
PDF	1.5
Lepton ID/isolation	2.0
Electron energy	0.4
b quark fragmentation	0.9
b tagging	1.2
Colour reconnection	1.4
Kinematic reconstruction	0.6
DY ME scale	0.4
Jet energy resolution	0.8
Muon energy scale	0.4
Pile-up	0.4
tW FSR scale	0.4
tW ISR scale	0.4
tW ME scale	0.4
m_{t}^{MC}	0.4
Top quark p_{T}	3.5
Trigger	0.5
b hadron BF	0.4
$\text{t}\bar{\text{t}}$ FSR scale	1.3
$\text{t}\bar{\text{t}}$ ISR scale	0.4
ME/PS matching	1.0
$\text{t}\bar{\text{t}}$ ME scale	1.8
UE tune	0.8
DY background	1.6
tW background	1.0
W+jets background	0.5
Diboson background	0.4
$\text{t}\bar{\text{t}}$ background	0.4
Integrated luminosity	2.6
Statistical	1.8
MC statistical	2.5
Extrapolation uncertainties	
$\text{t}\bar{\text{t}}$ ISR scale	$\mp_{0.7}^{0.8}$
$\text{t}\bar{\text{t}}$ FSR scale	$\pm_{<0.1}^{0.2}$
$\text{t}\bar{\text{t}}$ ME scale	$\mp_{1.2}^{0.8}$
UE tune	$\pm_{0.2}^{0.1}$
PDF	$\pm_{0.9}^{1.2}$
Top quark p_{T}	$\pm_{1.2}^{0.6}$
Total $\sigma_{\text{t}\bar{\text{t}}}^{(\mu_4)}$ uncertainty	$+7.2$ -6.9

B The CMS Collaboration

Yerevan Physics Institute, Yerevan, Armenia

A.M. Sirunyan[†], A. Tumasyan

Institut für Hochenergiephysik, Wien, Austria

W. Adam, F. Ambrogio, T. Bergauer, J. Brandstetter, M. Dragicevic, J. Erö, A. Escalante Del Valle, M. Flechl, R. Frühwirth¹, M. Jeitler¹, N. Krammer, I. Krätschmer, D. Liko, T. Madlener, I. Mikulec, N. Rad, J. Schieck¹, R. Schöfbeck, M. Spanring, D. Spitzbart, W. Waltenberger, C.-E. Wulz¹, M. Zarucki

Institute for Nuclear Problems, Minsk, Belarus

V. Drugakov, V. Mossolov, J. Suarez Gonzalez

Universiteit Antwerpen, Antwerpen, Belgium

M.R. Darwish, E.A. De Wolf, D. Di Croce, X. Janssen, A. Lelek, M. Pieters, H. Rejeb Sfar, H. Van Haevermaet, P. Van Mechelen, S. Van Putte, N. Van Remortel

Vrije Universiteit Brussel, Brussel, Belgium

F. Blekman, E.S. Bols, S.S. Chhibra, J. D'Hondt, J. De Clercq, D. Lontkovskyi, S. Lowette, I. Marchesini, S. Moortgat, Q. Python, K. Skovpen, S. Tavernier, W. Van Doninck, P. Van Mulders

Université Libre de Bruxelles, Bruxelles, Belgium

D. Beghin, B. Bilin, H. Brun, B. Clerbaux, G. De Lentdecker, H. Delannoy, B. Dorney, L. Favart, A. Grebenyuk, A.K. Kalsi, A. Popov, N. Postiau, E. Starling, L. Thomas, C. Vander Velde, P. Vanlaer, D. Vannerom

Ghent University, Ghent, Belgium

T. Cornelis, D. Dobur, I. Khvastunov², M. Niedziela, C. Roskas, M. Tytgat, W. Verbeke, B. Vermassen, M. Vit

Université Catholique de Louvain, Louvain-la-Neuve, Belgium

O. Bondu, G. Bruno, C. Caputo, P. David, C. Delaere, M. Delcourt, A. Giammanco, V. Lemaitre, J. Prisciandaro, A. Saggio, M. Vidal Marono, P. Vischia, J. Zobec

Centro Brasileiro de Pesquisas Físicas, Rio de Janeiro, Brazil

F.L. Alves, G.A. Alves, G. Correia Silva, C. Hensel, A. Moraes, P. Rebello Teles

Universidade do Estado do Rio de Janeiro, Rio de Janeiro, Brazil

E. Belchior Batista Das Chagas, W. Carvalho, J. Chinellato³, E. Coelho, E.M. Da Costa, G.G. Da Silveira⁴, D. De Jesus Damiao, C. De Oliveira Martins, S. Fonseca De Souza, L.M. Huertas Guativa, H. Malbouisson, J. Martins⁵, D. Matos Figueiredo, M. Medina Jaime⁶, M. Melo De Almeida, C. Mora Herrera, L. Mundim, H. Nogima, W.L. Prado Da Silva, L.J. Sanchez Rosas, A. Santoro, A. Sznajder, M. Thiel, E.J. Tonelli Manganote³, F. Torres Da Silva De Araujo, A. Vilela Pereira

Universidade Estadual Paulista ^a, Universidade Federal do ABC ^b, São Paulo, Brazil

C.A. Bernardes^a, L. Calligaris^a, T.R. Fernandez Perez Tomei^a, E.M. Gregores^b, D.S. Lemos, P.G. Mercadante^b, S.F. Novaes^a, SandraS. Padula^a

Institute for Nuclear Research and Nuclear Energy, Bulgarian Academy of Sciences, Sofia, Bulgaria

A. Aleksandrov, G. Antchev, R. Hadjiiska, P. Iaydjiev, M. Misheva, M. Rodozov, M. Shopova, G. Sultanov

University of Sofia, Sofia, Bulgaria

M. Bonchev, A. Dimitrov, T. Ivanov, L. Litov, B. Pavlov, P. Petkov

Beihang University, Beijing, China

W. Fang⁷, X. Gao⁷, L. Yuan

Institute of High Energy Physics, Beijing, China

G.M. Chen, H.S. Chen, M. Chen, C.H. Jiang, D. Leggat, H. Liao, Z. Liu, A. Spiezia, J. Tao, E. Yazgan, H. Zhang, S. Zhang⁸, J. Zhao

State Key Laboratory of Nuclear Physics and Technology, Peking University, Beijing, China

A. Agapitos, Y. Ban, G. Chen, A. Levin, J. Li, L. Li, Q. Li, Y. Mao, S.J. Qian, D. Wang, Q. Wang

Tsinghua University, Beijing, China

M. Ahmad, Z. Hu, Y. Wang

Zhejiang University, Hangzhou, China

M. Xiao

Universidad de Los Andes, Bogota, Colombia

C. Avila, A. Cabrera, C. Florez, C.F. González Hernández, M.A. Segura Delgado

Universidad de Antioquia, Medellin, Colombia

J. Mejia Guisao, J.D. Ruiz Alvarez, C.A. Salazar González, N. Vanegas Arbelaez

University of Split, Faculty of Electrical Engineering, Mechanical Engineering and Naval Architecture, Split, Croatia

D. Giljanović, N. Godinovic, D. Lelas, I. Puljak, T. Sculac

University of Split, Faculty of Science, Split, Croatia

Z. Antunovic, M. Kovac

Institute Rudjer Boskovic, Zagreb, Croatia

V. Brigljevic, D. Ferencek, K. Kadija, B. Mesic, M. Roguljic, A. Starodumov⁹, T. Susa

University of Cyprus, Nicosia, Cyprus

M.W. Ather, A. Attikis, E. Erodotos, A. Ioannou, M. Kolosova, S. Konstantinou, G. Mavromanolakis, J. Mousa, C. Nicolaou, F. Ptochos, P.A. Razis, H. Rykaczewski, D. Tsiakkouri

Charles University, Prague, Czech Republic

M. Finger¹⁰, M. Finger Jr.¹⁰, A. Kveton, J. Tomsa

Escuela Politecnica Nacional, Quito, Ecuador

E. Ayala

Universidad San Francisco de Quito, Quito, Ecuador

E. Carrera Jarrin

Academy of Scientific Research and Technology of the Arab Republic of Egypt, Egyptian Network of High Energy Physics, Cairo, Egypt

Y. Assran^{11,12}, S. Elgammal¹²

National Institute of Chemical Physics and Biophysics, Tallinn, Estonia

S. Bhowmik, A. Carvalho Antunes De Oliveira, R.K. Dewanjee, K. Ehataht, M. Kadastik, M. Raidal, C. Veelken

Department of Physics, University of Helsinki, Helsinki, Finland

P. Eerola, L. Forthomme, H. Kirschenmann, K. Osterberg, M. Voutilainen

Helsinki Institute of Physics, Helsinki, Finland

F. Garcia, J. Havukainen, J.K. Heikkilä, V. Karimäki, M.S. Kim, R. Kinnunen, T. Lampén, K. Lassila-Perini, S. Laurila, S. Lehti, T. Lindén, P. Luukka, T. Mäenpää, H. Siikonen, E. Tuominen, J. Tuominiemi

Lappeenranta University of Technology, Lappeenranta, Finland

T. Tuuva

IRFU, CEA, Université Paris-Saclay, Gif-sur-Yvette, France

M. Besancon, F. Couderc, M. Dejardin, D. Denegri, B. Fabbro, J.L. Faure, F. Ferri, S. Ganjour, A. Givernaud, P. Gras, G. Hamel de Monchenault, P. Jarry, C. Leloup, B. Lenzi, E. Locci, J. Malcles, J. Rander, A. Rosowsky, M.Ö. Sahin, A. Savoy-Navarro¹³, M. Titov, G.B. Yu

Laboratoire Leprince-Ringuet, CNRS/IN2P3, Ecole Polytechnique, Institut Polytechnique de Paris

S. Ahuja, C. Amendola, F. Beaudette, P. Busson, C. Charlot, B. Diab, G. Falmagne, R. Granier de Cassagnac, I. Kucher, A. Lobanov, C. Martin Perez, M. Nguyen, C. Ochando, P. Paganini, J. Rembser, R. Salerno, J.B. Sauvan, Y. Sirois, A. Zabi, A. Zghiche

Université de Strasbourg, CNRS, IPHC UMR 7178, Strasbourg, France

J.-L. Agram¹⁴, J. Andrea, D. Bloch, G. Bourgatte, J.-M. Brom, E.C. Chabert, C. Collard, E. Conte¹⁴, J.-C. Fontaine¹⁴, D. Gelé, U. Goerlach, M. Jansová, A.-C. Le Bihan, N. Tonon, P. Van Hove

Centre de Calcul de l'Institut National de Physique Nucleaire et de Physique des Particules, CNRS/IN2P3, Villeurbanne, France

S. Gadrat

Université de Lyon, Université Claude Bernard Lyon 1, CNRS-IN2P3, Institut de Physique Nucléaire de Lyon, Villeurbanne, France

S. Beauceron, C. Bernet, G. Boudoul, C. Camen, A. Carle, N. Chanon, R. Chierici, D. Contardo, P. Depasse, H. El Mamouni, J. Fay, S. Gascon, M. Gouzevitch, B. Ille, Sa. Jain, F. Lagarde, I.B. Laktineh, H. Lattaud, A. Lesauvage, M. Lethuillier, L. Mirabito, S. Perries, V. Sordini, L. Torterotot, G. Touquet, M. Vander Donckt, S. Viret

Georgian Technical University, Tbilisi, Georgia

T. Toriashvili¹⁵

Tbilisi State University, Tbilisi, Georgia

Z. Tsamalaidze¹⁰

RWTH Aachen University, I. Physikalisches Institut, Aachen, Germany

C. Autermann, L. Feld, M.K. Kiesel, K. Klein, M. Lipinski, D. Meuser, A. Pauls, M. Preuten, M.P. Rauch, J. Schulz, M. Teroerde, B. Wittmer

RWTH Aachen University, III. Physikalisches Institut A, Aachen, Germany

M. Erdmann, B. Fischer, S. Ghosh, T. Hebbeker, K. Hoepfner, H. Keller, L. Mastrolorenzo, M. Merschmeyer, A. Meyer, P. Millet, G. Mocellin, S. Mondal, S. Mukherjee, D. Noll, A. Novak, T. Pook, A. Pozdnyakov, T. Quast, M. Radziej, Y. Rath, H. Reithler, J. Roemer, A. Schmidt, S.C. Schuler, A. Sharma, S. Wiedenbeck, S. Zaleski

RWTH Aachen University, III. Physikalisches Institut B, Aachen, Germany

G. Flügge, W. Haj Ahmad¹⁶, O. Hlushchenko, T. Kress, T. Müller, A. Nowack, C. Pistone, O. Pooth, D. Roy, H. Sert, A. Stahl¹⁷

Deutsches Elektronen-Synchrotron, Hamburg, Germany

M. Aldaya Martin, P. Asmuss, I. Babounikau, H. Bakhshiansohi, K. Beernaert, O. Behnke, A. Bermúdez Martínez, D. Bertsche, A.A. Bin Anuar, K. Borras¹⁸, V. Botta, A. Campbell, A. Cardini, P. Connor, S. Consuegra Rodríguez, C. Contreras-Campana, V. Danilov, A. De Wit, M.M. Defranchis, C. Diez Pardos, D. Domínguez Damiani, G. Eckerlin, D. Eckstein, T. Eichhorn, A. Elwood, E. Eren, E. Gallo¹⁹, A. Geiser, A. Grohsjean, M. Guthoff, M. Haranko, A. Harb, A. Jafari, N.Z. Jomhari, H. Jung, A. Kasem¹⁸, M. Kasemann, H. Kaveh, J. Keaveney, C. Kleinwort, J. Knolle, D. Krücker, W. Lange, T. Lenz, J. Lidrych, K. Lipka, W. Lohmann²⁰, R. Mankel, I.-A. Melzer-Pellmann, A.B. Meyer, M. Meyer, M. Missiroli, G. Mittag, J. Mnich, S.O. Moch, A. Mussgiller, V. Myronenko, D. Pérez Adán, S.K. Pflitsch, D. Pitzl, A. Raspereza, A. Saibel, M. Savitskiy, V. Scheurer, P. Schütze, C. Schwanenberger, R. Shevchenko, A. Singh, H. Tholen, O. Turkot, A. Vagnerini, M. Van De Klundert, R. Walsh, Y. Wen, K. Wichmann, C. Wissing, O. Zenaiev, R. Zlebcik

University of Hamburg, Hamburg, Germany

R. Aggleton, S. Bein, L. Benato, A. Benecke, V. Blobel, T. Dreyer, A. Ebrahimi, F. Feindt, A. Fröhlich, C. Garbers, E. Garutti, D. Gonzalez, P. Gunnellini, J. Haller, A. Hinzmann, A. Karavdina, G. Kasieczka, R. Klanner, R. Kogler, N. Kovalchuk, S. Kurz, V. Kutzner, J. Lange, T. Lange, A. Malara, J. Multhaupt, C.E.N. Niemeyer, A. Perieanu, A. Reimers, O. Rieger, C. Scharf, P. Schleper, S. Schumann, J. Schwandt, J. Sonneveld, H. Stadie, G. Steinbrück, F.M. Stober, B. Vormwald, I. Zoi

Karlsruher Institut fuer Technologie, Karlsruhe, Germany

M. Akbiyik, C. Barth, M. Baselga, S. Baur, T. Berger, E. Butz, R. Caspart, T. Chwalek, W. De Boer, A. Dierlamm, K. El Morabit, N. Faltermann, M. Giffels, P. Goldenzweig, A. Gottmann, M.A. Harrendorf, F. Hartmann¹⁷, U. Husemann, S. Kudella, S. Mitra, M.U. Mozer, D. Müller, Th. Müller, M. Musich, A. Nürnberg, G. Quast, K. Rabbertz, M. Schröder, I. Shvetsov, H.J. Simonis, R. Ulrich, M. Wassmer, M. Weber, C. Wöhrmann, R. Wolf

Institute of Nuclear and Particle Physics (INPP), NCSR Demokritos, Aghia Paraskevi, Greece

G. Anagnostou, P. Asenov, G. Daskalakis, T. Geralis, A. Kyriakis, D. Loukas, G. Paspalaki

National and Kapodistrian University of Athens, Athens, Greece

M. Diamantopoulou, G. Karathanasis, P. Kontaxakis, A. Manousakis-katsikakis, A. Panagiotou, I. Papavergou, N. Saoulidou, A. Stakia, K. Theofilatos, K. Vellidis, E. Vourliotis

National Technical University of Athens, Athens, Greece

G. Bakas, K. Kousouris, I. Papakrivopoulos, G. Tsipolitis

University of Ioánnina, Ioánnina, Greece

I. Evangelou, C. Foudas, P. Giannelos, P. Katsoulis, P. Kokkas, S. Mallios, K. Manitará, N. Manthos, I. Papadopoulos, J. Strologas, F.A. Triantis, D. Tsitsonis

MTA-ELTE Lendület CMS Particle and Nuclear Physics Group, Eötvös Loránd University, Budapest, Hungary

M. Bartók²¹, R. Chudasama, M. Csanad, P. Major, K. Mandal, A. Mehta, M.I. Nagy, G. Pasztor, O. Surányi, G.I. Veres

Wigner Research Centre for Physics, Budapest, Hungary

G. Bencze, C. Hajdu, D. Horvath²², F. Sikler, T. Vámi, V. Veszpremi, G. Vesztergombi[†]

Institute of Nuclear Research ATOMKI, Debrecen, Hungary

N. Beni, S. Czellar, J. Karancsi²¹, A. Makovec, J. Molnar, Z. Szillasi

Institute of Physics, University of Debrecen, Debrecen, Hungary

P. Raics, D. Teyssier, Z.L. Trocsanyi, B. Ujvari

Eszterhazy Karoly University, Karoly Robert Campus, Gyongyos, Hungary

T. Csorgo, W.J. Metzger, F. Nemes, T. Novak

Indian Institute of Science (IISc), Bangalore, India

S. Choudhury, J.R. Komaragiri, P.C. Tiwari

National Institute of Science Education and Research, HBNI, Bhubaneswar, IndiaS. Bahinipati²⁴, C. Kar, G. Kole, P. Mal, V.K. Muraleedharan Nair Bindhu, A. Nayak²⁵, D.K. Sahoo²⁴, S.K. Swain**Panjab University, Chandigarh, India**

S. Bansal, S.B. Beri, V. Bhatnagar, S. Chauhan, R. Chawla, N. Dhingra, R. Gupta, A. Kaur, M. Kaur, S. Kaur, P. Kumari, M. Lohan, M. Meena, K. Sandeep, S. Sharma, J.B. Singh, A.K. Viridi

University of Delhi, Delhi, India

A. Bhardwaj, B.C. Choudhary, R.B. Garg, M. Gola, S. Keshri, Ashok Kumar, M. Naimuddin, P. Priyanka, K. Ranjan, Aashaq Shah, R. Sharma

Saha Institute of Nuclear Physics, HBNI, Kolkata, IndiaR. Bhardwaj²⁶, M. Bharti²⁶, R. Bhattacharya, S. Bhattacharya, U. Bhawandeep²⁶, D. Bhowmik, S. Dutta, S. Ghosh, B. Gomber²⁷, M. Maity²⁸, K. Mondal, S. Nandan, A. Purohit, P.K. Rout, G. Saha, S. Sarkar, T. Sarkar²⁸, M. Sharan, B. Singh²⁶, S. Thakur²⁶**Indian Institute of Technology Madras, Madras, India**

P.K. Behera, P. Kalbhor, A. Muhammad, P.R. Pujahari, A. Sharma, A.K. Sikdar

Bhabha Atomic Research Centre, Mumbai, India

D. Dutta, V. Jha, V. Kumar, D.K. Mishra, P.K. Netrakanti, L.M. Pant, P. Shukla

Tata Institute of Fundamental Research-A, Mumbai, India

T. Aziz, M.A. Bhat, S. Dugad, G.B. Mohanty, N. Sur, RavindraKumar Verma

Tata Institute of Fundamental Research-B, Mumbai, India

S. Banerjee, S. Bhattacharya, S. Chatterjee, P. Das, M. Guchait, S. Karmakar, S. Kumar, G. Majumder, K. Mazumdar, N. Sahoo, S. Sawant

Indian Institute of Science Education and Research (IISER), Pune, India

S. Dube, B. Kansal, A. Kapoor, K. Kothekar, S. Pandey, A. Rane, A. Rastogi, S. Sharma

Institute for Research in Fundamental Sciences (IPM), Tehran, IranS. Chenarani²⁹, E. Eskandari Tadavani, S.M. Etesami²⁹, M. Khakzad, M. Mohammadi Najafabadi, M. Naseri, F. Rezaei Hosseinabadi**University College Dublin, Dublin, Ireland**

M. Felcini, M. Grunewald

INFN Sezione di Bari ^a, Università di Bari ^b, Politecnico di Bari ^c, Bari, ItalyM. Abbrescia^{a,b}, R. Aly^{a,b,30}, C. Calabria^{a,b}, A. Colaleo^a, D. Creanza^{a,c}, L. Cristella^{a,b}, N. De Filippis^{a,c}, M. De Palma^{a,b}, A. Di Florio^{a,b}, W. Elmetenawee^{a,b}, L. Fiore^a, A. Gelmi^{a,b}, G. Iaselli^{a,c}, M. Ince^{a,b}, S. Lezki^{a,b}, G. Maggi^{a,c}, M. Maggi^a, J.A. Merlin, G. Miniello^{a,b}, S. My^{a,b}, S. Nuzzo^{a,b}, A. Pompili^{a,b}, G. Pugliese^{a,c}, R. Radogna^a, A. Ranieri^a, G. Selvaggi^{a,b}, L. Silvestris^a, F.M. Simone^{a,b}, R. Venditti^a, P. Verwilligen^a

INFN Sezione di Bologna ^a, Università di Bologna ^b, Bologna, Italy

G. Abbiendi^a, C. Battilana^{a,b}, D. Bonacorsi^{a,b}, L. Borgonovi^{a,b}, S. Braibant-Giacomelli^{a,b}, R. Campanini^{a,b}, P. Capiluppi^{a,b}, A. Castro^{a,b}, F.R. Cavallo^a, C. Ciocca^a, G. Codispoti^{a,b}, M. Cuffiani^{a,b}, G.M. Dallavalle^a, F. Fabbri^a, A. Fanfani^{a,b}, E. Fontanesi^{a,b}, P. Giacomelli^a, C. Grandi^a, L. Guiducci^{a,b}, F. Iemmi^{a,b}, S. Lo Meo^{a,31}, S. Marcellini^a, G. Masetti^a, F.L. Navarria^{a,b}, A. Perrotta^a, F. Primavera^{a,b}, A.M. Rossi^{a,b}, T. Rovelli^{a,b}, G.P. Siroli^{a,b}, N. Tosi^a

INFN Sezione di Catania ^a, Università di Catania ^b, Catania, Italy

S. Albergo^{a,b,32}, S. Costa^{a,b}, A. Di Mattia^a, R. Potenza^{a,b}, A. Tricomi^{a,b,32}, C. Tuve^{a,b}

INFN Sezione di Firenze ^a, Università di Firenze ^b, Firenze, Italy

G. Barbagli^a, A. Cassese, R. Ceccarelli, V. Ciulli^{a,b}, C. Civinini^a, R. D'Alessandro^{a,b}, F. Fiori^{a,c}, E. Focardi^{a,b}, G. Latino^{a,b}, P. Lenzi^{a,b}, M. Meschini^a, S. Paoletti^a, G. Sguazzoni^a, L. Viliani^a

INFN Laboratori Nazionali di Frascati, Frascati, Italy

L. Benussi, S. Bianco, D. Piccolo

INFN Sezione di Genova ^a, Università di Genova ^b, Genova, Italy

M. Bozzo^{a,b}, F. Ferro^a, R. Mulargia^{a,b}, E. Robutti^a, S. Tosi^{a,b}

INFN Sezione di Milano-Bicocca ^a, Università di Milano-Bicocca ^b, Milano, Italy

A. Benaglia^a, A. Beschi^{a,b}, F. Brivio^{a,b}, V. Ciriolo^{a,b,17}, S. Di Guida^{a,b,17}, M.E. Dinardo^{a,b}, P. Dini^a, S. Gennai^a, A. Ghezzi^{a,b}, P. Govoni^{a,b}, L. Guzzi^{a,b}, M. Malberti^a, S. Malvezzi^a, D. Menasce^a, F. Monti^{a,b}, L. Moroni^a, M. Paganoni^{a,b}, D. Pedrini^a, S. Ragazzi^{a,b}, T. Tabarelli de Fatis^{a,b}, D. Zuolo^{a,b}

INFN Sezione di Napoli ^a, Università di Napoli 'Federico II' ^b, Napoli, Italy, Università della Basilicata ^c, Potenza, Italy, Università G. Marconi ^d, Roma, Italy

S. Buontempo^a, N. Cavallo^{a,c}, A. De Iorio^{a,b}, A. Di Crescenzo^{a,b}, F. Fabozzi^{a,c}, F. Fienga^a, G. Galati^a, A.O.M. Iorio^{a,b}, L. Lista^{a,b}, S. Meola^{a,d,17}, P. Paolucci^{a,17}, B. Rossi^a, C. Sciacca^{a,b}, E. Voevodina^{a,b}

INFN Sezione di Padova ^a, Università di Padova ^b, Padova, Italy, Università di Trento ^c, Trento, Italy

P. Azzi^a, N. Bacchetta^a, D. Bisello^{a,b}, A. Boletti^{a,b}, A. Bragagnolo^{a,b}, R. Carlin^{a,b}, P. Checchia^a, P. De Castro Manzano^a, T. Dorigo^a, U. Dosselli^a, F. Gasparini^{a,b}, U. Gasparini^{a,b}, A. Gozzelino^a, S.Y. Hoh^{a,b}, P. Lujan^a, M. Margoni^{a,b}, A.T. Meneguzzo^{a,b}, J. Pazzini^{a,b}, M. Presilla^b, P. Ronchese^{a,b}, R. Rossin^{a,b}, F. Simonetto^{a,b}, A. Tiko^a, M. Tosi^{a,b}, M. Zanetti^{a,b}, P. Zotto^{a,b}, G. Zumerle^{a,b}

INFN Sezione di Pavia ^a, Università di Pavia ^b, Pavia, Italy

A. Braghieri^a, D. Fiorina^{a,b}, P. Montagna^{a,b}, S.P. Ratti^{a,b}, V. Re^a, M. Ressegotti^{a,b}, C. Riccardi^{a,b}, P. Salvini^a, I. Vai^a, P. Vitulo^{a,b}

INFN Sezione di Perugia ^a, Università di Perugia ^b, Perugia, Italy

M. Biasini^{a,b}, G.M. Bilei^a, D. Ciangottini^{a,b}, L. Fanò^{a,b}, P. Lariccia^{a,b}, R. Leonardi^{a,b}, E. Manoni^a, G. Mantovani^{a,b}, V. Mariani^{a,b}, M. Menichelli^a, A. Rossi^{a,b}, A. Santocchia^{a,b}, D. Spiga^a

INFN Sezione di Pisa ^a, Università di Pisa ^b, Scuola Normale Superiore di Pisa ^c, Pisa, Italy

K. Androsov^a, P. Azzurri^a, G. Bagliesi^a, V. Bertacchi^{a,c}, L. Bianchini^a, T. Boccali^a, R. Castaldi^a, M.A. Ciocci^{a,b}, R. Dell'Orso^a, S. Donato^a, G. Fedi^a, L. Giannini^{a,c}, A. Giassi^a, M.T. Grippo^a, F. Ligabue^{a,c}, E. Manca^{a,c}, G. Mandorli^{a,c}, A. Messineo^{a,b}, F. Palla^a, A. Rizzi^{a,b}, G. Rolandi³³, S. Roy Chowdhury, A. Scribano^a, P. Spagnolo^a, R. Tenchini^a, G. Tonelli^{a,b}, N. Turini, A. Venturi^a, P.G. Verdini^a

INFN Sezione di Roma ^a, Sapienza Università di Roma ^b, Rome, Italy

F. Cavallari^a, M. Cipriani^{a,b}, D. Del Re^{a,b}, E. Di Marco^a, M. Diemoz^a, E. Longo^{a,b}, P. Meridiani^a, G. Organtini^{a,b}, F. Pandolfi^a, R. Paramatti^{a,b}, C. Quaranta^{a,b}, S. Rahatlou^{a,b}, C. Rovelli^a, F. Santanastasio^{a,b}, L. Soffi^{a,b}

INFN Sezione di Torino ^a, Università di Torino ^b, Torino, Italy, Università del Piemonte Orientale ^c, Novara, Italy

N. Amapane^{a,b}, R. Arcidiacono^{a,c}, S. Argiro^{a,b}, M. Arneodo^{a,c}, N. Bartosik^a, R. Bellan^{a,b}, A. Bellora, C. Biino^a, A. Cappati^{a,b}, N. Cartiglia^a, S. Cometti^a, M. Costa^{a,b}, R. Covarelli^{a,b}, N. Demaria^a, B. Kiani^{a,b}, F. Legger, C. Mariotti^a, S. Maselli^a, E. Migliore^{a,b}, V. Monaco^{a,b}, E. Monteil^{a,b}, M. Monteno^a, M.M. Obertino^{a,b}, G. Ortona^{a,b}, L. Pacher^{a,b}, N. Pastrone^a, M. Pelliccioni^a, G.L. Pinna Angioni^{a,b}, A. Romero^{a,b}, M. Ruspa^{a,c}, R. Salvatico^{a,b}, V. Sola^a, A. Solano^{a,b}, D. Soldi^{a,b}, A. Staiano^a, D. Trocino^{a,b}

INFN Sezione di Trieste ^a, Università di Trieste ^b, Trieste, Italy

S. Belforte^a, V. Candelise^{a,b}, M. Casarsa^a, F. Cossutti^a, A. Da Rold^{a,b}, G. Della Ricca^{a,b}, F. Vazzoler^{a,b}, A. Zanetti^a

Kyungpook National University, Daegu, Korea

B. Kim, D.H. Kim, G.N. Kim, J. Lee, S.W. Lee, C.S. Moon, Y.D. Oh, S.I. Pak, S. Sekmen, D.C. Son, Y.C. Yang

Chonnam National University, Institute for Universe and Elementary Particles, Kwangju, Korea

H. Kim, D.H. Moon, G. Oh

Hanyang University, Seoul, Korea

B. Francois, T.J. Kim, J. Park

Korea University, Seoul, Korea

S. Cho, S. Choi, Y. Go, S. Ha, B. Hong, K. Lee, K.S. Lee, J. Lim, J. Park, S.K. Park, Y. Roh, J. Yoo

Kyung Hee University, Department of Physics

J. Goh

Sejong University, Seoul, Korea

H.S. Kim

Seoul National University, Seoul, Korea

J. Almond, J.H. Bhyun, J. Choi, S. Jeon, J. Kim, J.S. Kim, H. Lee, K. Lee, S. Lee, K. Nam, M. Oh, S.B. Oh, B.C. Radburn-Smith, U.K. Yang, H.D. Yoo, I. Yoon

University of Seoul, Seoul, Korea

D. Jeon, J.H. Kim, J.S.H. Lee, I.C. Park, I.J. Watson

Sungkyunkwan University, Suwon, Korea

Y. Choi, C. Hwang, Y. Jeong, J. Lee, Y. Lee, I. Yu

Riga Technical University, Riga, Latvia

V. Veckalns³⁴

Vilnius University, Vilnius, Lithuania

V. Dudenas, A. Juodagalvis, A. Rinkevicius, G. Tamulaitis, J. Vaitkus

National Centre for Particle Physics, Universiti Malaya, Kuala Lumpur, Malaysia

Z.A. Ibrahim, F. Mohamad Idris³⁵, W.A.T. Wan Abdullah, M.N. Yusli, Z. Zolkapli

Universidad de Sonora (UNISON), Hermosillo, Mexico

J.F. Benitez, A. Castaneda Hernandez, J.A. Murillo Quijada, L. Valencia Palomo

Centro de Investigacion y de Estudios Avanzados del IPN, Mexico City, Mexico

H. Castilla-Valdez, E. De La Cruz-Burelo, I. Heredia-De La Cruz³⁶, R. Lopez-Fernandez, A. Sanchez-Hernandez

Universidad Iberoamericana, Mexico City, Mexico

S. Carrillo Moreno, C. Oropeza Barrera, M. Ramirez-Garcia, F. Vazquez Valencia

Benemerita Universidad Autonoma de Puebla, Puebla, Mexico

J. Eysermans, I. Pedraza, H.A. Salazar Ibarguen, C. Uribe Estrada

Universidad Autónoma de San Luis Potosí, San Luis Potosí, Mexico

A. Morelos Pineda

University of Montenegro, Podgorica, Montenegro

J. Mijuskovic², N. Raicevic

University of Auckland, Auckland, New Zealand

D. Krofcheck

University of Canterbury, Christchurch, New Zealand

S. Bheesette, P.H. Butler

National Centre for Physics, Quaid-I-Azam University, Islamabad, Pakistan

A. Ahmad, M. Ahmad, Q. Hassan, H.R. Hoorani, W.A. Khan, M.A. Shah, M. Shoaib, M. Waqas

AGH University of Science and Technology Faculty of Computer Science, Electronics and Telecommunications, Krakow, Poland

V. Avati, L. Grzanka, M. Malawski

National Centre for Nuclear Research, Swierk, Poland

H. Bialkowska, M. Bluj, B. Boimska, M. Górski, M. Kazana, M. Szeleper, P. Zalewski

Institute of Experimental Physics, Faculty of Physics, University of Warsaw, Warsaw, Poland

K. Bunkowski, A. Byszuk³⁷, K. Doroba, A. Kalinowski, M. Konecki, J. Krolikowski, M. Olszewski, M. Walczak

Laboratório de Instrumentação e Física Experimental de Partículas, Lisboa, Portugal

M. Araujo, P. Bargassa, D. Bastos, A. Di Francesco, P. Faccioli, B. Galinhas, M. Gallinaro, J. Hollar, N. Leonardo, T. Niknejad, J. Seixas, K. Shchelina, G. Strong, O. Toldaiev, J. Varela

Joint Institute for Nuclear Research, Dubna, Russia

S. Afanasiev, P. Bunin, M. Gavrilenko, I. Golutvin, I. Gorbunov, A. Kamenev, V. Karjavine, A. Lanev, A. Malakhov, V. Matveev^{38,39}, P. Moiseenz, V. Palichik, V. Perelygin, M. Savina, S. Shmatov, S. Shulha, N. Skatchkov, V. Smirnov, N. Voytishin, A. Zarubin

Petersburg Nuclear Physics Institute, Gatchina (St. Petersburg), Russia

L. Chtchypounov, V. Golovtcov, Y. Ivanov, V. Kim⁴⁰, E. Kuznetsova⁴¹, P. Levchenko, V. Murzin, V. Oreshkin, I. Smirnov, D. Sosnov, V. Sulimov, L. Uvarov, A. Vorobyev

Institute for Nuclear Research, Moscow, Russia

Yu. Andreev, A. Dermenev, S. Gninenko, N. Golubev, A. Karneyeu, M. Kirsanov, N. Krasnikov, A. Pashenkov, D. Tlisov, A. Toropin

Institute for Theoretical and Experimental Physics named by A.I. Alikhanov of NRC 'Kurchatov Institute', Moscow, Russia

V. Epshteyn, V. Gavrilov, N. Lychkovskaya, A. Nikitenko⁴², V. Popov, I. Pozdnyakov, G. Safronov, A. Spiridonov, A. Stepenov, M. Toms, E. Vlasov, A. Zhokin

Moscow Institute of Physics and Technology, Moscow, Russia

T. Aushev

National Research Nuclear University 'Moscow Engineering Physics Institute' (MEPhI), Moscow, Russia

O. Bychkova, R. Chistov⁴³, M. Danilov⁴³, S. Polikarpov⁴³, E. Tarkovskii

P.N. Lebedev Physical Institute, Moscow, Russia

V. Andreev, M. Azarkin, I. Dremin, M. Kirakosyan, A. Terkulov

Skobeltsyn Institute of Nuclear Physics, Lomonosov Moscow State University, Moscow, Russia

A. Baskakov, A. Belyaev, E. Boos, V. Bunichev, M. Dubinin⁴⁴, L. Dudko, V. Klyukhin, O. Kodolova, N. Korneeva, I. Lokhtin, S. Obraztsov, M. Perfilov, V. Savrin

Novosibirsk State University (NSU), Novosibirsk, Russia

A. Barnyakov⁴⁵, V. Blinov⁴⁵, T. Dimova⁴⁵, L. Kardapoltsev⁴⁵, Y. Skovpen⁴⁵

Institute for High Energy Physics of National Research Centre 'Kurchatov Institute', Protvino, Russia

I. Azhgirey, I. Bayshev, S. Bitioukov, V. Kachanov, D. Konstantinov, P. Mandrik, V. Petrov, R. Ryutin, S. Slabospitskii, A. Sobol, S. Troshin, N. Tyurin, A. Uzunian, A. Volkov

National Research Tomsk Polytechnic University, Tomsk, Russia

A. Babaev, A. Iuzhakov, V. Okhotnikov

Tomsk State University, Tomsk, Russia

V. Borchsh, V. Ivanchenko, E. Tcherniaev

University of Belgrade: Faculty of Physics and VINCA Institute of Nuclear Sciences

P. Adzic⁴⁶, P. Cirkovic, M. Dordevic, P. Milenovic, J. Milosevic, M. Stojanovic

Centro de Investigaciones Energéticas Medioambientales y Tecnológicas (CIEMAT), Madrid, Spain

M. Aguilar-Benitez, J. Alcaraz Maestre, A. Alvarez Fernández, I. Bachiller, M. Barrio Luna, Cristina F. Bedoya, J.A. Brochero Cifuentes, C.A. Carrillo Montoya, M. Cepeda, M. Cerrada, N. Colino, B. De La Cruz, A. Delgado Peris, J.P. Fernández Ramos, J. Flix, M.C. Fouz, O. Gonzalez Lopez, S. Goy Lopez, J.M. Hernandez, M.I. Josa, D. Moran, . Navarro Tobar, A. Pérez-Calero Yzquierdo, J. Puerta Pelayo, I. Redondo, L. Romero, S. Sánchez Navas, M.S. Soares, A. Triossi, C. Willmott

Universidad Autónoma de Madrid, Madrid, Spain

C. Albajar, J.F. de Trocóniz, R. Reyes-Almanza

Universidad de Oviedo, Instituto Universitario de Ciencias y Tecnologías Espaciales de Asturias (ICTEA), Oviedo, Spain

B. Alvarez Gonzalez, J. Cuevas, C. Erice, J. Fernandez Menendez, S. Folgueras, I. Gonzalez Caballero, J.R. González Fernández, E. Palencia Cortezon, V. Rodríguez Bouza, S. Sanchez Cruz

Instituto de Física de Cantabria (IFCA), CSIC-Universidad de Cantabria, Santander, Spain

I.J. Cabrillo, A. Calderon, B. Chazin Quero, J. Duarte Campderros, M. Fernandez,

P.J. Fernández Manteca, A. García Alonso, G. Gomez, C. Martinez Rivero, P. Martinez Ruiz del Arbol, F. Matorras, J. Piedra Gomez, C. Prieels, T. Rodrigo, A. Ruiz-Jimeno, L. Russo⁴⁷, L. Scodellaro, I. Vila, J.M. Vizan Garcia

University of Colombo, Colombo, Sri Lanka

K. Malagalage

University of Ruhuna, Department of Physics, Matara, Sri Lanka

W.G.D. Dharmaratna, N. Wickramage

CERN, European Organization for Nuclear Research, Geneva, Switzerland

D. Abbaneo, B. Akgun, E. Auffray, G. Auzinger, J. Baechler, P. Baillon, A.H. Ball, D. Barney, J. Bendavid, M. Bianco, A. Bocci, P. Bortignon, E. Bossini, C. Botta, E. Brondolin, T. Camporesi, A. Caratelli, G. Cerminara, E. Chapon, G. Cucciati, D. d'Enterria, A. Dabrowski, N. Daci, V. Daponte, A. David, O. Davignon, A. De Roeck, M. Deile, M. Dobson, M. Dünser, N. Dupont, A. Elliott-Peisert, N. Emriskova, F. Fallavollita⁴⁸, D. Fasanella, S. Fiorendi, G. Franzoni, J. Fulcher, W. Funk, S. Giani, D. Gigi, A. Gilbert, K. Gill, F. Glege, L. Gouskos, M. Gruchala, M. Guilbaud, D. Gulhan, J. Hegeman, C. Heidegger, Y. Iiyama, V. Innocente, T. James, P. Janot, O. Karacheban²⁰, J. Kaspar, J. Kieseler, M. Krammer¹, N. Kratochwil, C. Lange, P. Lecoq, C. Lourenço, L. Malgeri, M. Mannelli, A. Massironi, F. Meijers, S. Mersi, E. Meschi, F. Moortgat, M. Mulders, J. Ngadiuba, J. Niedziela, S. Nourbakhsh, S. Orfanelli, L. Orsini, F. Pantaleo¹⁷, L. Pape, E. Perez, M. Peruzzi, A. Petrilli, G. Petrucciani, A. Pfeiffer, M. Pierini, F.M. Pitters, D. Rabady, A. Racz, M. Rieger, M. Rovere, H. Sakulin, J. Salfeld-Nebgen, C. Schäfer, C. Schwick, M. Selvaggi, A. Sharma, P. Silva, W. Snoeys, P. Sphicas⁴⁹, J. Steggemann, S. Summers, V.R. Tavolaro, D. Treille, A. Tsirou, G.P. Van Onsem, A. Vartak, M. Verzetti, W.D. Zeuner

Paul Scherrer Institut, Villigen, Switzerland

L. Caminada⁵⁰, K. Deiters, W. Erdmann, R. Horisberger, Q. Ingram, H.C. Kaestli, D. Kotlinski, U. Langenegger, T. Rohe, S.A. Wiederkehr

ETH Zurich - Institute for Particle Physics and Astrophysics (IPA), Zurich, Switzerland

M. Backhaus, P. Berger, N. Chernyavskaya, G. Dissertori, M. Dittmar, M. Donegà, C. Dorfer, T.A. Gómez Espinosa, C. Grab, D. Hits, W. Lusterhmann, R.A. Manzoni, M.T. Meinhard, F. Micheli, P. Musella, F. Nessi-Tedaldi, F. Pauss, G. Perrin, L. Perrozzi, S. Pigazzini, M.G. Ratti, M. Reichmann, C. Reissel, T. Reitenspiess, B. Ristic, D. Ruini, D.A. Sanz Becerra, M. Schönenberger, L. Shchutska, M.L. Vesterbacka Olsson, R. Wallny, D.H. Zhu

Universität Zürich, Zurich, Switzerland

T.K. Aarrestad, C. AMSler⁵¹, D. Brzhechko, M.F. Canelli, A. De Cosa, R. Del Burgo, B. Kilminster, S. Leontsinis, V.M. Mikuni, I. Neutelings, G. Rauco, P. Robmann, K. Schweiger, C. Seitz, Y. Takahashi, S. Wertz, A. Zucchetta

National Central University, Chung-Li, Taiwan

T.H. Doan, C.M. Kuo, W. Lin, A. Roy, S.S. Yu

National Taiwan University (NTU), Taipei, Taiwan

P. Chang, Y. Chao, K.F. Chen, P.H. Chen, W.-S. Hou, Y.y. Li, R.-S. Lu, E. Paganis, A. Psallidas, A. Steen

Chulalongkorn University, Faculty of Science, Department of Physics, Bangkok, Thailand

B. Asavapibhop, C. Asawatangtrakuldee, N. Srimanobhas, N. Suwonjandee

ukurova University, Physics Department, Science and Art Faculty, Adana, Turkey

A. Bat, F. Boran, A. Celik⁵², S. Cerci⁵³, S. Damarseckin⁵⁴, Z.S. Demiroglu, F. Dolek, C. Dozen⁵⁵,

I. Dumanoglu, G. Gokbulut, EmineGurpinar Guler⁵⁶, Y. Guler, I. Hos⁵⁷, C. Isik, E.E. Kangal⁵⁸, O. Kara, A. Kayis Topaksu, U. Kiminsu, G. Onengut, K. Ozdemir⁵⁹, S. Ozturk⁶⁰, A.E. Simsek, D. Sunar Cerci⁵³, U.G. Tok, S. Turkcapar, I.S. Zorbakir, C. Zorbilmez

Middle East Technical University, Physics Department, Ankara, Turkey

B. Isildak⁶¹, G. Karapinar⁶², M. Yalvac

Bogazici University, Istanbul, Turkey

I.O. Atakisi, E. Gülmez, M. Kaya⁶³, O. Kaya⁶⁴, Ö. Özçelik, S. Tekten, E.A. Yetkin⁶⁵

Istanbul Technical University, Istanbul, Turkey

A. Cakir, K. Cankocak, Y. Komurcu, S. Sen⁶⁶

Istanbul University, Istanbul, Turkey

B. Kaynak, S. Ozkorucuklu

Institute for Scintillation Materials of National Academy of Science of Ukraine, Kharkov, Ukraine

B. Grynyov

National Scientific Center, Kharkov Institute of Physics and Technology, Kharkov, Ukraine

L. Levchuk

University of Bristol, Bristol, United Kingdom

E. Bhal, S. Bologna, J.J. Brooke, D. Burns⁶⁷, E. Clement, D. Cussans, H. Flacher, J. Goldstein, G.P. Heath, H.F. Heath, L. Kreczko, B. Krikler, S. Paramesvaran, B. Penning, T. Sakuma, S. Seif El Nasr-Storey, V.J. Smith, J. Taylor, A. Titterton

Rutherford Appleton Laboratory, Didcot, United Kingdom

K.W. Bell, A. Belyaev⁶⁸, C. Brew, R.M. Brown, D.J.A. Cockerill, J.A. Coughlan, K. Harder, S. Harper, J. Linacre, K. Manolopoulos, D.M. Newbold, E. Olaiya, D. Petyt, T. Reis, T. Schuh, C.H. Shepherd-Themistocleous, A. Thea, I.R. Tomalin, T. Williams, W.J. Womersley

Imperial College, London, United Kingdom

R. Bainbridge, P. Bloch, J. Borg, S. Breeze, O. Buchmuller, A. Bundock, GurpreetSingh CHAHAL⁶⁹, D. Colling, P. Dauncey, G. Davies, M. Della Negra, R. Di Maria, P. Everaerts, G. Hall, G. Iles, M. Komm, C. Laner, L. Lyons, A.-M. Magnan, S. Malik, A. Martelli, V. Milosevic, A. Morton, J. Nash⁷⁰, V. Palladino, M. Pesaresi, D.M. Raymond, A. Richards, A. Rose, E. Scott, C. Seez, A. Shtipliyski, M. Stoye, T. Strebler, A. Tapper, K. Uchida, T. Virdee¹⁷, N. Wardle, D. Winterbottom, J. Wright, A.G. Zecchinelli, S.C. Zenz

Brunel University, Uxbridge, United Kingdom

J.E. Cole, P.R. Hobson, A. Khan, P. Kyberd, C.K. Mackay, I.D. Reid, L. Teodorescu, S. Zahid

Baylor University, Waco, USA

K. Call, B. Caraway, J. Dittmann, K. Hatakeyama, C. Madrid, B. McMaster, N. Pastika, C. Smith

Catholic University of America, Washington, DC, USA

R. Bartek, A. Dominguez, R. Uniyal, A.M. Vargas Hernandez

The University of Alabama, Tuscaloosa, USA

A. Buccilli, S.I. Cooper, C. Henderson, P. Rumerio, C. West

Boston University, Boston, USA

A. Albert, D. Arcaro, Z. Demiragli, D. Gastler, C. Richardson, J. Rohlf, D. Sperka, I. Suarez, L. Sulak, D. Zou

Brown University, Providence, USA

G. Benelli, B. Burkler, X. Coubez¹⁸, D. Cutts, Y.t. Duh, M. Hadley, U. Heintz, J.M. Hogan⁷¹, K.H.M. Kwok, E. Laird, G. Landsberg, K.T. Lau, J. Lee, Z. Mao, M. Narain, S. Sagir⁷², R. Syarif, E. Usai, W.Y. Wong, D. Yu, W. Zhang

University of California, Davis, Davis, USA

R. Band, C. Brainerd, R. Breedon, M. Calderon De La Barca Sanchez, M. Chertok, J. Conway, R. Conway, P.T. Cox, R. Erbacher, C. Flores, G. Funk, F. Jensen, W. Ko, O. Kukral, R. Lander, M. Mulhearn, D. Pellett, J. Pilot, M. Shi, D. Taylor, K. Tos, M. Tripathi, Z. Wang, F. Zhang

University of California, Los Angeles, USA

M. Bachtis, C. Bravo, R. Cousins, A. Dasgupta, A. Florent, J. Hauser, M. Ignatenko, N. Mccoll, W.A. Nash, S. Regnard, D. Saltzberg, C. Schnaible, B. Stone, V. Valuev

University of California, Riverside, Riverside, USA

K. Burt, Y. Chen, R. Clare, J.W. Gary, S.M.A. Ghiasi Shirazi, G. Hanson, G. Karapostoli, E. Kennedy, O.R. Long, M. Olmedo Negrete, M.I. Paneva, W. Si, L. Wang, S. Wimpenny, B.R. Yates, Y. Zhang

University of California, San Diego, La Jolla, USA

J.G. Branson, P. Chang, S. Cittolin, S. Cooperstein, N. Deelen, M. Derdzinski, R. Gerosa, D. Gilbert, B. Hashemi, D. Klein, V. Krutelyov, J. Letts, M. Masciovecchio, S. May, S. Padhi, M. Pieri, V. Sharma, M. Tadel, F. Würthwein, A. Yagil, G. Zevi Della Porta

University of California, Santa Barbara - Department of Physics, Santa Barbara, USA

N. Amin, R. Bhandari, C. Campagnari, M. Citron, V. Dutta, M. Franco Sevilla, J. Incandela, B. Marsh, H. Mei, A. Ovcharova, H. Qu, J. Richman, U. Sarica, D. Stuart, S. Wang

California Institute of Technology, Pasadena, USA

D. Anderson, A. Bornheim, O. Cerri, I. Dutta, J.M. Lawhorn, N. Lu, J. Mao, H.B. Newman, T.Q. Nguyen, J. Pata, M. Spiropulu, J.R. Vlimant, S. Xie, Z. Zhang, R.Y. Zhu

Carnegie Mellon University, Pittsburgh, USA

M.B. Andrews, T. Ferguson, T. Mudholkar, M. Paulini, M. Sun, I. Vorobiev, M. Weinberg

University of Colorado Boulder, Boulder, USA

J.P. Cumalat, W.T. Ford, E. MacDonald, T. Mulholland, R. Patel, A. Perloff, K. Stenson, K.A. Ulmer, S.R. Wagner

Cornell University, Ithaca, USA

J. Alexander, Y. Cheng, J. Chu, A. Datta, A. Frankenthal, K. Mcdermott, J.R. Patterson, D. Quach, A. Ryd, S.M. Tan, Z. Tao, J. Thom, P. Wittich, M. Zientek

Fermi National Accelerator Laboratory, Batavia, USA

S. Abdullin, M. Albrow, M. Alyari, G. Apollinari, A. Apresyan, A. Apyan, S. Banerjee, L.A.T. Bauerdick, A. Beretvas, D. Berry, J. Berryhill, P.C. Bhat, K. Burkett, J.N. Butler, A. Canepa, G.B. Cerati, H.W.K. Cheung, F. Chlebana, M. Cremonesi, J. Duarte, V.D. Elvira, J. Freeman, Z. Gecse, E. Gottschalk, L. Gray, D. Green, S. Grünendahl, O. Gutsche, AllisonReinsvold Hall, J. Hanlon, R.M. Harris, S. Hasegawa, R. Heller, J. Hirschauer, B. Jayatilaka, S. Jindariani, M. Johnson, U. Joshi, T. Klijnsma, B. Klima, M.J. Kortelainen, B. Kreis, S. Lammel, J. Lewis, D. Lincoln, R. Lipton, M. Liu, T. Liu, J. Lykken, K. Maeshima, J.M. Marraffino, D. Mason, P. McBride, P. Merkel, S. Mrenna, S. Nahn, V. O'Dell, V. Papadimitriou, K. Pedro, C. Pena, G. Rakness, F. Ravera, L. Ristori, B. Schneider, E. Sexton-Kennedy, N. Smith, A. Soha,

W.J. Spalding, L. Spiegel, S. Stoynev, J. Strait, N. Strobbe, L. Taylor, S. Tkaczyk, N.V. Tran, L. Uplegger, E.W. Vaandering, C. Vernieri, R. Vidal, M. Wang, H.A. Weber

University of Florida, Gainesville, USA

D. Acosta, P. Avery, D. Bourilkov, A. Brinkerhoff, L. Cadamuro, A. Carnes, V. Cherepanov, F. Errico, R.D. Field, S.V. Gleyzer, D. Guerrero, B.M. Joshi, M. Kim, J. Konigsberg, A. Korytov, K.H. Lo, P. Ma, K. Matchev, N. Menendez, G. Mitselmakher, D. Rosenzweig, K. Shi, J. Wang, S. Wang, X. Zuo

Florida International University, Miami, USA

Y.R. Joshi

Florida State University, Tallahassee, USA

T. Adams, A. Askew, S. Hagopian, V. Hagopian, K.F. Johnson, R. Khurana, T. Kolberg, G. Martinez, T. Perry, H. Prosper, C. Schiber, R. Yohay, J. Zhang

Florida Institute of Technology, Melbourne, USA

M.M. Baarmand, M. Hohlmann, D. Noonan, M. Rahmani, M. Saunders, F. Yumiceva

University of Illinois at Chicago (UIC), Chicago, USA

M.R. Adams, L. Apanasevich, R.R. Betts, R. Cavanaugh, X. Chen, S. Dittmer, O. Evdokimov, C.E. Gerber, D.A. Hangal, D.J. Hofman, K. Jung, C. Mills, T. Roy, M.B. Tonjes, N. Varelas, J. Viinikainen, H. Wang, X. Wang, Z. Wu

The University of Iowa, Iowa City, USA

M. Alhusseini, B. Bilki⁵⁶, W. Clarida, K. Dilsiz⁷³, S. Durgut, R.P. Gandrajula, M. Haytmyradov, V. Khristenko, O.K. Köseyan, J.-P. Merlo, A. Mestvirishvili⁷⁴, A. Moeller, J. Nachtman, H. Ogul⁷⁵, Y. Onel, F. Ozok⁷⁶, A. Penzo, C. Snyder, E. Tiras, J. Wetzel

Johns Hopkins University, Baltimore, USA

B. Blumenfeld, A. Cocoros, N. Eminizer, A.V. Gritsan, W.T. Hung, S. Kyriacou, P. Maksimovic, J. Roskes, M. Swartz

The University of Kansas, Lawrence, USA

C. Baldenegro Barrera, P. Baringer, A. Bean, S. Boren, J. Bowen, A. Bylinkin, T. Isidori, S. Khalil, J. King, G. Krintiras, A. Kropivnitskaya, C. Lindsey, D. Majumder, W. Mcbrayer, N. Minafra, M. Murray, C. Rogan, C. Royon, S. Sanders, E. Schmitz, J.D. Tapia Takaki, Q. Wang, J. Williams, G. Wilson

Kansas State University, Manhattan, USA

S. Duric, A. Ivanov, K. Kaadze, D. Kim, Y. Maravin, D.R. Mendis, T. Mitchell, A. Modak, A. Mohammadi

Lawrence Livermore National Laboratory, Livermore, USA

F. Rebassoo, D. Wright

University of Maryland, College Park, USA

A. Baden, O. Baron, A. Belloni, S.C. Eno, Y. Feng, N.J. Hadley, S. Jabeen, G.Y. Jeng, R.G. Kellogg, J. Kunkle, A.C. Mignerey, S. Nabili, F. Ricci-Tam, Y.H. Shin, A. Skuja, S.C. Tonwar, K. Wong

Massachusetts Institute of Technology, Cambridge, USA

D. Abercrombie, B. Allen, A. Baty, R. Bi, S. Brandt, W. Busza, I.A. Cali, M. D'Alfonso, G. Gomez Ceballos, M. Goncharov, P. Harris, D. Hsu, M. Hu, M. Klute, D. Kovalskyi, Y.-J. Lee, P.D. Luckey, B. Maier, A.C. Marini, C. McGinn, C. Mironov, S. Narayanan, X. Niu, C. Paus,

D. Rankin, C. Roland, G. Roland, Z. Shi, G.S.F. Stephans, K. Sumorok, K. Tatar, D. Velicanu, J. Wang, T.W. Wang, B. Wyslouch

University of Minnesota, Minneapolis, USA

R.M. Chatterjee, A. Evans, S. Guts[†], P. Hansen, J. Hiltbrand, Sh. Jain, Y. Kubota, Z. Lesko, J. Mans, M. Revering, R. Rusack, R. Saradhy, N. Schroeder, M.A. Wadud

University of Mississippi, Oxford, USA

J.G. Acosta, S. Oliveros

University of Nebraska-Lincoln, Lincoln, USA

K. Bloom, S. Chauhan, D.R. Claes, C. Fangmeier, L. Finco, F. Golf, R. Kamalieddin, I. Kravchenko, J.E. Siado, G.R. Snow[†], B. Stieger, W. Tabb

State University of New York at Buffalo, Buffalo, USA

G. Agarwal, C. Harrington, I. Iashvili, A. Kharchilava, C. McLean, D. Nguyen, A. Parker, J. Pekkanen, S. Rappoccio, B. Roozbahani

Northeastern University, Boston, USA

G. Alverson, E. Barberis, C. Freer, Y. Haddad, A. Hortiangtham, G. Madigan, B. Marzocchi, D.M. Morse, T. Orimoto, L. Skinnari, A. Tishelman-Charny, T. Wamorkar, B. Wang, A. Wisecarver, D. Wood

Northwestern University, Evanston, USA

S. Bhattacharya, J. Bueghly, T. Gunter, K.A. Hahn, N. Odell, M.H. Schmitt, K. Sung, M. Trovato, M. Velasco

University of Notre Dame, Notre Dame, USA

R. Bucci, N. Dev, R. Goldouzian, M. Hildreth, K. Hurtado Anampa, C. Jessop, D.J. Karmgard, K. Lannon, W. Li, N. Loukas, N. Marinelli, I. Mcalister, F. Meng, C. Mueller, Y. Musienko³⁸, M. Planer, R. Ruchti, P. Siddireddy, G. Smith, S. Taroni, M. Wayne, A. Wightman, M. Wolf, A. Woodard

The Ohio State University, Columbus, USA

J. Alimena, B. Bylsma, L.S. Durkin, B. Francis, C. Hill, W. Ji, A. Lefeld, T.Y. Ling, B.L. Winer

Princeton University, Princeton, USA

G. Dezoort, P. Elmer, J. Hardenbrook, N. Haubrich, S. Higginbotham, A. Kalogeropoulos, S. Kwan, D. Lange, M.T. Lucchini, J. Luo, D. Marlow, K. Mei, I. Ojalvo, J. Olsen, C. Palmer, P. Piroué, D. Stickland, C. Tully, Z. Wang

University of Puerto Rico, Mayaguez, USA

S. Malik, S. Norberg

Purdue University, West Lafayette, USA

A. Barker, V.E. Barnes, S. Das, L. Gutay, M. Jones, A.W. Jung, A. Khatiwada, B. Mahakud, D.H. Miller, G. Negro, N. Neumeister, C.C. Peng, S. Piperov, H. Qiu, J.F. Schulte, N. Trevisani, F. Wang, R. Xiao, W. Xie

Purdue University Northwest, Hammond, USA

T. Cheng, J. Dolen, N. Parashar

Rice University, Houston, USA

U. Behrens, K.M. Ecklund, S. Freed, F.J.M. Geurts, M. Kilpatrick, Arun Kumar, W. Li, B.P. Padley, R. Redjimi, J. Roberts, J. Rorie, W. Shi, A.G. Stahl Leiton, Z. Tu, A. Zhang

University of Rochester, Rochester, USA

A. Bodek, P. de Barbaro, R. Demina, J.L. Dulemba, C. Fallon, T. Ferbel, M. Galanti, A. Garcia-Bellido, O. Hindrichs, A. Khukhunaishvili, E. Ranken, R. Taus

Rutgers, The State University of New Jersey, Piscataway, USA

B. Chiarito, J.P. Chou, A. Gandrakota, Y. Gershtein, E. Halkiadakis, A. Hart, M. Heindl, E. Hughes, S. Kaplan, I. Laflotte, A. Lath, R. Montalvo, K. Nash, M. Osherson, H. Saka, S. Salur, S. Schnetzer, S. Somalwar, R. Stone, S. Thomas

University of Tennessee, Knoxville, USA

H. Acharya, A.G. Delannoy, S. Spanier

Texas A&M University, College Station, USA

O. Bouhali⁷⁷, M. Dalchenko, M. De Mattia, A. Delgado, S. Dildick, R. Eusebi, J. Gilmore, T. Huang, T. Kamon⁷⁸, H. Kim, S. Luo, S. Malhotra, D. Marley, R. Mueller, D. Overton, L. Perniè, D. Rathjens, A. Safonov

Texas Tech University, Lubbock, USA

N. Akchurin, J. Damgov, F. De Guio, V. Hegde, S. Kunori, K. Lamichhane, S.W. Lee, T. Mengke, S. Muthumuni, T. Peltola, S. Undleeb, I. Volobouev, Z. Wang, A. Whitbeck

Vanderbilt University, Nashville, USA

S. Greene, A. Gurrola, R. Janjam, W. Johns, C. Maguire, A. Melo, H. Ni, K. Padeken, F. Romeo, P. Sheldon, S. Tuo, J. Velkovska, M. Verweij

University of Virginia, Charlottesville, USA

M.W. Arenton, P. Barria, B. Cox, G. Cummings, J. Hakala, R. Hirosky, M. Joyce, A. Ledovskoy, C. Neu, B. Tannenwald, Y. Wang, E. Wolfe, F. Xia

Wayne State University, Detroit, USA

R. Harr, P.E. Karchin, N. Poudyal, J. Sturdy, P. Thapa

University of Wisconsin - Madison, Madison, WI, USA

T. Bose, J. Buchanan, C. Caillol, D. Carlsmith, S. Dasu, I. De Bruyn, L. Dodd, C. Galloni, H. He, M. Herndon, A. Hervé, U. Hussain, P. Klabbers, A. Lanaro, A. Loeliger, K. Long, R. Loveless, J. Madhusudanan Sreekala, D. Pinna, T. Ruggles, A. Savin, V. Sharma, W.H. Smith, D. Teague, S. Trembath-reichert, N. Woods

†: Deceased

1: Also at Vienna University of Technology, Vienna, Austria

2: Also at IRFU, CEA, Université Paris-Saclay, Gif-sur-Yvette, France

3: Also at Universidade Estadual de Campinas, Campinas, Brazil

4: Also at Federal University of Rio Grande do Sul, Porto Alegre, Brazil

5: Also at UFMS, Nova Andradina, Brazil

6: Also at Universidade Federal de Pelotas, Pelotas, Brazil

7: Also at Université Libre de Bruxelles, Bruxelles, Belgium

8: Also at University of Chinese Academy of Sciences, Beijing, China

9: Also at Institute for Theoretical and Experimental Physics named by A.I. Alikhanov of NRC 'Kurchatov Institute', Moscow, Russia

10: Also at Joint Institute for Nuclear Research, Dubna, Russia

11: Also at Suez University, Suez, Egypt

12: Now at British University in Egypt, Cairo, Egypt

13: Also at Purdue University, West Lafayette, USA

14: Also at Université de Haute Alsace, Mulhouse, France

- 15: Also at Tbilisi State University, Tbilisi, Georgia
- 16: Also at Erzincan Binali Yildirim University, Erzincan, Turkey
- 17: Also at CERN, European Organization for Nuclear Research, Geneva, Switzerland
- 18: Also at RWTH Aachen University, III. Physikalisches Institut A, Aachen, Germany
- 19: Also at University of Hamburg, Hamburg, Germany
- 20: Also at Brandenburg University of Technology, Cottbus, Germany
- 21: Also at Institute of Physics, University of Debrecen, Debrecen, Hungary, Debrecen, Hungary
- 22: Also at Institute of Nuclear Research ATOMKI, Debrecen, Hungary
- 23: Also at MTA-ELTE Lendület CMS Particle and Nuclear Physics Group, Eötvös Loránd University, Budapest, Hungary, Budapest, Hungary
- 24: Also at IIT Bhubaneswar, Bhubaneswar, India, Bhubaneswar, India
- 25: Also at Institute of Physics, Bhubaneswar, India
- 26: Also at Shoolini University, Solan, India
- 27: Also at University of Hyderabad, Hyderabad, India
- 28: Also at University of Visva-Bharati, Santiniketan, India
- 29: Also at Isfahan University of Technology, Isfahan, Iran
- 30: Now at INFN Sezione di Bari ^a, Università di Bari ^b, Politecnico di Bari ^c, Bari, Italy
- 31: Also at Italian National Agency for New Technologies, Energy and Sustainable Economic Development, Bologna, Italy
- 32: Also at Centro Siciliano di Fisica Nucleare e di Struttura Della Materia, Catania, Italy
- 33: Also at Scuola Normale e Sezione dell'INFN, Pisa, Italy
- 34: Also at Riga Technical University, Riga, Latvia, Riga, Latvia
- 35: Also at Malaysian Nuclear Agency, MOSTI, Kajang, Malaysia
- 36: Also at Consejo Nacional de Ciencia y Tecnología, Mexico City, Mexico
- 37: Also at Warsaw University of Technology, Institute of Electronic Systems, Warsaw, Poland
- 38: Also at Institute for Nuclear Research, Moscow, Russia
- 39: Now at National Research Nuclear University 'Moscow Engineering Physics Institute' (MEPhI), Moscow, Russia
- 40: Also at St. Petersburg State Polytechnical University, St. Petersburg, Russia
- 41: Also at University of Florida, Gainesville, USA
- 42: Also at Imperial College, London, United Kingdom
- 43: Also at P.N. Lebedev Physical Institute, Moscow, Russia
- 44: Also at California Institute of Technology, Pasadena, USA
- 45: Also at Budker Institute of Nuclear Physics, Novosibirsk, Russia
- 46: Also at Faculty of Physics, University of Belgrade, Belgrade, Serbia
- 47: Also at Università degli Studi di Siena, Siena, Italy
- 48: Also at INFN Sezione di Pavia ^a, Università di Pavia ^b, Pavia, Italy, Pavia, Italy
- 49: Also at National and Kapodistrian University of Athens, Athens, Greece
- 50: Also at Universität Zürich, Zurich, Switzerland
- 51: Also at Stefan Meyer Institute for Subatomic Physics, Vienna, Austria, Vienna, Austria
- 52: Also at Burdur Mehmet Akif Ersoy University, BURDUR, Turkey
- 53: Also at Adiyaman University, Adiyaman, Turkey
- 54: Also at Şırnak University, Sirnak, Turkey
- 55: Also at Tsinghua University, Beijing, China
- 56: Also at Beykent University, Istanbul, Turkey, Istanbul, Turkey
- 57: Also at Istanbul Aydın University, Istanbul, Turkey
- 58: Also at Mersin University, Mersin, Turkey
- 59: Also at Piri Reis University, Istanbul, Turkey

- 60: Also at Gaziosmanpasa University, Tokat, Turkey
- 61: Also at Ozyegin University, Istanbul, Turkey
- 62: Also at Izmir Institute of Technology, Izmir, Turkey
- 63: Also at Marmara University, Istanbul, Turkey
- 64: Also at Kafkas University, Kars, Turkey
- 65: Also at Istanbul Bilgi University, Istanbul, Turkey
- 66: Also at Hacettepe University, Ankara, Turkey
- 67: Also at Vrije Universiteit Brussel, Brussel, Belgium
- 68: Also at School of Physics and Astronomy, University of Southampton, Southampton, United Kingdom
- 69: Also at IPPP Durham University, Durham, United Kingdom
- 70: Also at Monash University, Faculty of Science, Clayton, Australia
- 71: Also at Bethel University, St. Paul, Minneapolis, USA, St. Paul, USA
- 72: Also at Karamanoğlu Mehmetbey University, Karaman, Turkey
- 73: Also at Bingol University, Bingol, Turkey
- 74: Also at Georgian Technical University, Tbilisi, Georgia
- 75: Also at Sinop University, Sinop, Turkey
- 76: Also at Mimar Sinan University, Istanbul, Istanbul, Turkey
- 77: Also at Texas A&M University at Qatar, Doha, Qatar
- 78: Also at Kyungpook National University, Daegu, Korea, Daegu, Korea